



저작자표시-비영리-변경금지 2.0 대한민국

이용자는 아래의 조건을 따르는 경우에 한하여 자유롭게

- 이 저작물을 복제, 배포, 전송, 전시, 공연 및 방송할 수 있습니다.

다음과 같은 조건을 따라야 합니다:



저작자표시. 귀하는 원저작자를 표시하여야 합니다.



비영리. 귀하는 이 저작물을 영리 목적으로 이용할 수 없습니다.



변경금지. 귀하는 이 저작물을 개작, 변형 또는 가공할 수 없습니다.

- 귀하는, 이 저작물의 재이용이나 배포의 경우, 이 저작물에 적용된 이용허락조건을 명확하게 나타내어야 합니다.
- 저작권자로부터 별도의 허가를 받으면 이러한 조건들은 적용되지 않습니다.

저작권법에 따른 이용자의 권리는 위의 내용에 의하여 영향을 받지 않습니다.

이것은 [이용허락규약\(Legal Code\)](#)을 이해하기 쉽게 요약한 것입니다.

[Disclaimer](#)

Ph. D Thesis
박사 학위논문

Roles of palmitate in regulation of autophagy and
ER stress in hypothalamic cells

Yun Lim (임 윤 林 潤)

Department of
Brain and Cognitive Sciences

DGIST

2021

Ph. D Thesis
박사 학위논문

Roles of palmitate in regulation of autophagy and
ER stress in hypothalamic cells

Yun Lim (임 윤 林 潤)

Department of
Brain and Cognitive Sciences

DGIST

2021

Roles of palmitate in regulation of autophagy and ER stress in hypothalamic cells

Advisor: Professor Eun-Kyoung Kim

Co-advisor: Professor Myungjin Kim

by

Yun Lim

Department of Brain and Cognitive Sciences

DGIST

A thesis submitted to the faculty of DGIST in partial fulfillment of the requirements for the degree of Doctor of Philosophy in the Department of Brain and Cognitive Sciences. The study was conducted in accordance with Code of Research Ethics¹

5. 24. 2021

Approved by

Professor Eun-Kyoung Kim
(Advisor)



Professor Myungjin Kim
(Co-Advisor)



¹ Declaration of Ethical Conduct in Research: I, as a graduate student of DGIST, hereby declare that I have not committed any acts that may damage the credibility of my research. These include, but are not limited to: falsification, thesis written by someone else, distortion of research findings or plagiarism. I affirm that my thesis contains honest conclusions based on my own careful research under the guidance of my thesis advisor.

Roles of palmitate in regulation of autophagy and ER stress in hypothalamic cells

Yun Lim

Accepted in partial fulfillment of the requirements for the degree of Doctor of Philosophy.

5. 24. 2021

Head of Committee Prof. Seong-Woon Yu 

Committee Member Prof. Eun-Kyoung Kim 

Committee Member Prof. Myungjin Kim 

Committee Member Prof. Kyuhyung Kim 

Committee Member Prof. Sung Bae Lee 

Ph.D/BS
201325010

임 윤. Yun Lim. Roles of palmitate in regulation of autophagy and ER stress in hypothalamic cells. Department of Brain and Cognitive Sciences. 2021. 63p. Advisors Prof. Eun-Kyoung Kim, Co-Advisors Prof. Myungjin Kim

ABSTRACT

Palmitate is a saturated fatty acid that is well known to induce endoplasmic reticulum (ER) stress and autophagy. A high-fat diet (HFD) increases the palmitate level in the hypothalamus, the main region of the brain regulating energy metabolism, and induces lipotoxic inflammation related to obesity and type 2 diabetes mellitus. Interestingly, hypothalamic palmitate level is also increased under starvation, demanding the study to distinguish the effects of elevated hypothalamic palmitate level under different nutrient conditions. Herein, I show that ER-phagy (ER-targeted selective autophagy) is an antecedent to ER stress and that palmitate decreases ER stress by inhibiting ER-phagy in hypothalamic cells under starvation conditions. Palmitate inhibited starvation-induced ER-phagy by increasing the level of B-cell lymphoma 2 (Bcl-2) protein, which inhibits autophagy initiation. These findings suggest that palmitate, unlike increases ER stress under nutrient-rich conditions, decreases ER stress in hypothalamic cells by inhibiting ER-phagy under starvation conditions.

Keywords: Palmitate, Autophagy, ER-phagy, ER stress, Hypothalamus

List of Contents

Abstract	i
List of contents	ii
List of tables	iv
List of figures	v
List of abbreviations	vii
I. Introduction	1
1. Hypothalamus	1
2. Palmitate	1
2.1 Regulation of palmitate in high-fat diet	1
2.2 Regulation of palmitate under starvation	2
3. ER stress	4
4. Autophagy	6
4.1 Macroautophagy	6
4.2 Selective autophagy: ER-phagy	9
5. Aims of the study	11
II. Materials and methods	12
1. Cell culture	12
2. Preparation of palmitate	12
3. siRNA and plasmid transfection	12
4. Immunocytochemistry	13
5. Antibodies and chemical reagents	13
6. Western blotting	14

7. RNA extraction and quantitative Real time-PCR	15
8. Statistical analysis.....	15
III. Results	17
1. Palmitate induces ER stress.....	17
2. Palmitate induces autophagy in a short time treatment but the prolonged treatment of palmitate impairs autophagy	20
3. Palmitate impairs ER-phagy at the autophagosome maturation step	23
4. Palmitate does not induce mitophagy	26
5. Short-term treatment with palmitate inhibits ER-phagy under starvation	29
6. ER-phagy precedes ER stress and palmitate reduces ER stress by inhibiting ER-phagy under starvation	33
7. Palmitate inhibits ER-phagy at the initiation step under starvation.....	37
8. Inhibition of Bcl-2 ameliorates the inhibitory effect of palmitate on ER-phagy under starvation	41
IV. Discussion	46
V. Conclusion	51
VI. References	52
Abstract in Korean	62

List of Tables

Table 1. Sequences of primers used for qRT-PCR	16
--	----

List of Figures

Figure 1. The effect of palmitate on hypothalamic cells in HFD and starvation.	3
Figure 2. The activation of UPR pathways response to ER stress.	5
Figure 3. The process of autophagy.	8
Figure 4. The model for ER-phagy.	10
Figure 5. The effect of palmitate on ER stress in different time points and doses in hypothalamic N41 cells	18
Figure 6. Palmitate induces ER stress in N41 cells.	19
Figure 7. Palmitate induces autophagy at early time points, but prolonged treatment of palmitate impairs autophagy in N41 cells.	22
Figure 8. The effect of palmitate on ER-phagy receptors in N41 cells.	24
Figure 9. Palmitate impairs ER-phagy in N41 cells.	25
Figure 10. Palmitate dose not induce recruitment of parkin to mitochondria in N41 cells.	27
Figure 11. Palmitate does not accumulate COX IV in N41 cells.	28
Figure 12. Palmitate inhibits EBSS-induced colocalization of mRFP-GFP and KDEL in N41 cells.	30
Figure 13. Palmitate blocks EBSS-induced ER-phagy in N41 cells.	32
Figure 14. Palmitate inhibits EBSS-induced ER stress in N41 cells.	34
Figure 15. Inhibitory effect of palmitate on EBSS-induced ER-phagy precedes EBSS-induced ER stress in N41 cells.	35
Figure 16. Palmitate inhibits EBSS-induced increase of the number of mRFP-LC3 puncta in N41 cells.	38
Figure 17. Palmitate inhibits EBSS-induced increase of the number of mRFP-LC3 puncta in N41 cells.	39
Figure 18. Palmitate does not change the levels of ATG5 and ATG7 in N41 cells.	40
Figure 19. Palmitate increases the levels of Bcl-2 and Beclin1 under starvation in N41 cells.	

.....42

Figure 20. Palmitate does not increase the levels of Bcl-2 and Beclin1 after knockdown of *Bcl-2* under starvation in N41 cells.43

Figure 21. Palmitate inhibits ER-phagy via upregulating of Bcl-2 in N41 cells.44

Figure 22. The mRNA level of *Beclin1* is not changed by palmitate and/or EBSS in N41 cells.45

Figure 23. A Schematic diagram illustrating the different roles of palmitate in ER-phagy and ER stress under nutrient-rich and starvation conditions.50

List of Abbreviations

4PBA	Sodium phenylbutyrate
ATF4	Activating transcription factor 4
ATF6	Activating transcription factor 6
Atg	Autophagy-related
Baf A1	Bafilomycin A ₁
Bcl-2	B-cell lymphoma-2
CCCP	Carbonyl cyanide m-chlorophenylhydrazone
CCPG1	Cell cycle progression gene 1
CHOP	CCAAT/enhancer-binding protein homologous protein
COX IV	Cytochrome c oxidase subunit 4
DFCP1	Double FYVE-domain-containing protein 1
EBSS	Free fatty acid
ER	Endoplasmic reticulum
FFA	Earle's balanced salt solution
FIP200	FAK family-interacting protein of 200 kDa
GFP	Green fluorescent protein
HFD	High-fat diet
IRE1	Inositol-requiring transmembrane kinase/endonuclease 1
LC3	Microtubule-associated protein 1 light chain 3
NBR1	Neighbor of BRCA1 gene
PRKN/Parkin	Parkin RBR E3 ubiquitin protein ligase
PD	Parkinson's disease

PERK	Pancreatic ER kinase
RFP	Red fluorescent protein
RTN3	Reticulon 3
siRNA	Small interfering RNA
p62/SQSTM1	p62/Sequestosome 1
ULK1	Unc-51 like autophagy activating kinase 1
UPR	Unfolded protein response
XBP1	X-Box Binding Protein 1

I. INTRODUCTION

1. Hypothalamus

The hypothalamus is a brain region crucial for maintaining energy homeostasis by regulating food intake and energy expenditure (Minokoshi et al., 2004; Sainsbury et al., 2002; Williams et al., 2001). To control energy homeostasis, hypothalamic energy centers gather nutritional information to integrate metabolic signals including nutrients such as glucose and fatty acids, and hormones such as leptin, ghrelin, and insulin (Schwartz et al., 2000; Waterson and Horvath, 2015). Among them, free fatty acids (FFAs) cause not only insulin resistance or leptin resistance, but also hypothalamic inflammation which is one of the reasons for metabolic diseases such as obesity and diabetes (Boden and Shulman, 2002; Hernández-Cáceres et al., 2019; Ishii et al., 2015; Mayer and Belsham, 2010).

2. Palmitate

2.1 Regulation of palmitate in high-fat diet

Consumption of high-fat diet (HFD) is one of the major factors leading to the development of obesity and related complications. HFD-induced obesity is characterized by increased circulating free fatty acids, which are derived from adipocytes through lipolysis (Boden and Shulman, 2002). Specifically, the level of palmitate, a 16-carbon saturated fatty acid, is increased in the brain of both obese mice and humans (Gimenez da Silva-Santi et al., 2018; Melo et al., 2020). Since excessive palmitate induces lipotoxicity linked to obesity pathology (Dalvi et al., 2017), palmitate has been used in diet-induced obesity model at the cellular and organismal levels. HFD or administration of palmitate significantly reduces insulin activity and induces hypothalamic inflammation (Benoit et

al., 2009; Maric et al., 2014; Moraes et al., 2009), resulting in the development of obesity. Studies using hypothalamic cell lines have revealed that palmitate directly modulates diverse cellular processes including insulin and leptin resistance, endoplasmic reticulum (ER) stress, and apoptosis (Choi et al., 2010; Mayer and Belsham, 2010; Milanski et al., 2009; Oh et al., 2019; Tse and Belsham, 2018), all of which affects hypothalamic functions (Fig. 1).

2.2 Regulation of palmitate under starvation

Similar to HFD-induced obesity, fasting in a healthy state also increases the level of plasma FFAs (Sprangers et al., 2001), including palmitate, which arise from the hydrolysis of triglycerides in adipocytes (Park et al., 2019). During starvation, circulating FFAs are used as a primary fuel to maintain cellular energy status through fatty acid oxidation in most peripheral tissues including liver, muscle, and kidney (Lee et al., 2016; Marvyn et al., 2015; Weigle et al., 1998), indicating the role of fasting FFAs as a nutritional source. Fasting-induced circulating FFAs reach the hypothalamus across the blood–brain barrier (Hamilton and Brunaldi, 2007; Pardridge and Mietus, 1980). They are rapidly taken up by hypothalamic neurons where they are initially esterified to triglycerides within lipid droplets and then broken down by autophagy, which in turn induces appetite-regulating neuropeptide expression (Kaushik et al., 2011; Park et al., 2019). However, the role of increased hypothalamic palmitate in response to fasting conditions, beyond regulation of neuropeptide expression, is not fully elucidated (Fig. 1).

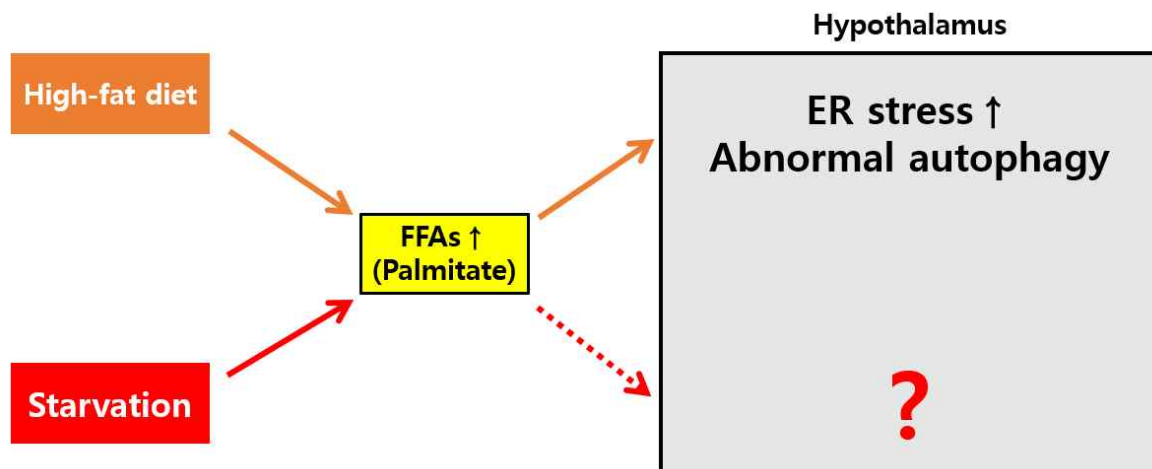


Figure 1. The effect of palmitate on hypothalamic cells in HFD and starvation. HFD-raised FFAs induce ER stress and abnormal autophagy in the hypothalamus. Starvation also raises the level of FFAs, but the effect of starvation-increased FFAs on hypothalamic ER stress and autophagy is not well revealed yet.

3. Endoplasmic reticulum (ER) stress

Stimuli such as aggregated proteins or unfolded proteins in the ER lumen provoke the unfolded protein response (UPR) to handle ER stress. There are three UPR sensors with distinct activation mechanisms: pancreatic ER kinase (PERK), inositol-requiring transmembrane kinase/endonuclease 1 (IRE1), and activating transcription factor 6 (ATF6). Phosphorylated PERK (p-PERK) activates activating transcription factor 4 (ATF4), and ATF4 activates CCAAT/enhancer-binding protein-homologous protein (CHOP). Phosphorylated IRE1 (p-IRE1) phosphorylates c-Jun N-terminal kinase, which activates CHOP. ER stress induces the transcription factor domain of ATF6 to enter the nucleus and regulate transcription of UPR target genes (Fig. 2). The three sensors activate different pathways but also activate common adaptive processes for cell survival such as autophagy (Kouroku et al., 2007; Liu et al., 2020; Sharma et al., 2017).

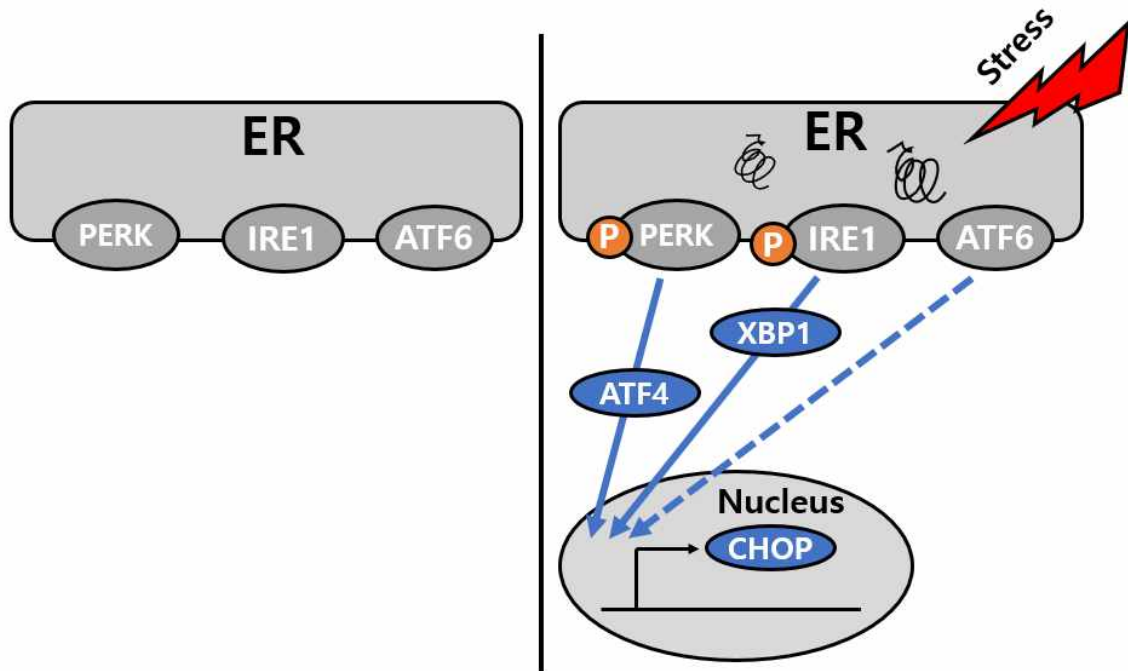


Figure 2. The activation of UPR pathways response to ER stress. During unstressed conditions (left panel), unfolded protein response (UPR) transmembrane proteins are inactivated: pancreatic ER kinase (PERK), inositol-requiring transmembrane kinase/endonuclease 1 (IRE1), and activating transcription factor 6 (ATF6). When unfolded proteins accumulate by ER stress (right panel). PERK is activated by phosphorylation. Phosphorylated PERK leads translocation of ATF4 to the nucleus, where it activates CHOP. IRE1 is activated by phosphorylation. Phosphorylated IRE1 activates CHOP by splicing XBP1 mRNA. ATF6 induces transcription of CHOP.

4. Autophagy

4.1 Macroautophagy

Macroautophagy (hereafter autophagy) is a lysosomal pathway for the degradation of aggregated proteins and damaged organelles to maintain cellular homeostasis (Levine and Klionsky, 2004; Mizushima et al., 2008). Autophagy participates in a variety of cellular physiological processes such as lipid metabolism (Singh et al., 2009), glucose homeostasis (Kotoulas et al., 2006), and aging (Cuervo, 2008; Cuervo et al., 2005; Rubinsztein et al., 2011). Cellular dysfunctions are often caused by the failure of autophagy to remove defective proteins or damaged organelles. In *Caenorhabditis elegans*, premature aging occurs when autophagy is inhibited (Toth et al., 2008). In contrast, enhanced autophagy extends the lifespan of *Drosophila melanogaster* (Simonsen et al., 2008). Deletion of the autophagy-related (Atg) gene family provokes an imbalance of body homeostasis, resulting in insulin resistance (Yang et al., 2010), obesity (Meng and Cai, 2011), diabetes (Jung and Lee, 2010), and neurodegeneration (Komatsu et al., 2006).

Among all types of cells, neurons are easily damaged by impaired autophagy (Hara et al., 2006; Komatsu et al., 2006). Neurons that lack of autophagy have a problem to maintain axonal homeostasis (Komatsu et al., 2007) and synaptic activity (Hernandez et al., 2012). Neurodegenerative diseases are typically irreversible and prevalent in the aged population. However, some food types like HFD may cause memory deficit in young age (Alzoubi et al., 2009; Greenwood and Winocur, 2001). Some metabolic dysfunctions are linked to neurodegenerative diseases such as Alzheimer's disease, Parkinson's disease (PD) and Huntington's disease. For example, PD is significantly correlated with diabetes (Sandyk, 1993) and increased iron deposition in neurons (Ayton et al., 2015).

Autophagy occurs through distinct steps (Fig. 3). When organelles are damaged or proteins are aggregated, those substrates are enclosed in autophagosomes and autophagosomes encounter lyso-

somes via a series of specific processes to produce autolysosomes. The formation of autophagosomes is initiated during the early stages of autophagy by the ULK1/Atg13/FIP200 kinase complex, which triggers the formation of a phagophore, the initial form of autophagosome (Hosokawa et al., 2009). Beclin1, the mammalian orthologue of yeast Atg6, also participates in the formation of autophagosomes by forming a complex with Vps34 when the Bcl-2/Beclin 1 complex dissociates (Kihara et al., 2001; Pattingre et al., 2005b). The origin of the autophagosomal membrane is still controversial, with the mitochondria (Cook et al., 2014; Hailey et al., 2010; Reggiori et al., 2005), ER (Axe et al., 2008a; Ueno et al., 1991; Yla-Anttila et al., 2009), and Golgi (Geng et al., 2010; Guo et al., 2012; van der Vaart et al., 2010) being the main candidates. Microtubule-associated protein light chain 3 (LC3) is converted into LC3-I by Atg4 (Kabeya et al., 2000). Then LC3-I is conjugated with phosphatidylethanolamine, forming LC3-II by Atg7, an E1 enzyme and Atg3, an E2 protein (Ichimura et al., 2000). Adaptor proteins such as p62/sequestosome 1, NBR1 and NDP52 (Kirkin et al., 2009; Pankiv et al., 2007; Thurston et al., 2009) anchor substrates of autophagy to LC3-II. Subsequently, misfolded protein (Rabinowitz and White, 2010) or abnormal cellular organelles including mitochondria (Geisler et al., 2010), ER (Bernales et al., 2007), or peroxisome (Kim et al., 2008) are engulfed by double-membrane autophagosome. The autophagosomes are fused with a lysosome, forming an autolysosome where the entrapped substrates are degraded (Kirkin et al., 2009; Pankiv et al., 2007; Thurston et al., 2009).

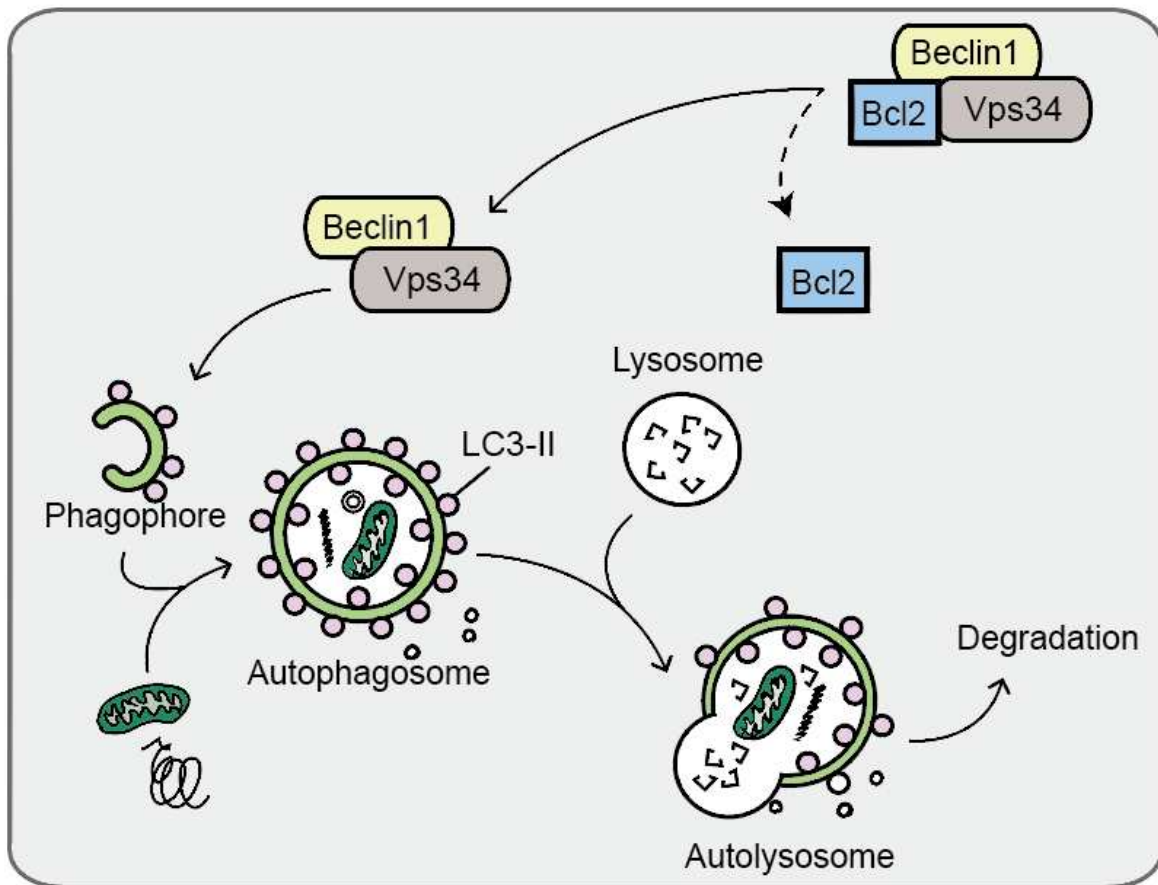


Figure 3. The process of autophagy. Bcl-2 inhibits autophagy by binding with Beclin1 that forms a complex with Vps34. When Bcl2 is dissociated from complex, beclin1 leads to initiate the formation of autophagosome. LC3-II positive phagophores sequester some portions of cytosol such as misfolded proteins or abnormal organelles and form an autophagosome. The outer membrane of the autophagosome subsequently fuses with the lysosome, and the internal material is degraded in the autolysosome.

4.2 Selective autophagy: ER-phagy

Autophagy is usually considered as a non-selective process; however, the selective clearance of specific cellular organelles such as lipid droplets, mitochondria, nuclei, peroxisomes, and ER through autophagy, called selective autophagy, has been discovered (Cho et al., 2018; Khaminets et al., 2015; Kim et al., 2020; Papandreou and Tavernarakis, 2019; Vives-Bauza et al., 2010). Among them, the term ER-phagy is firstly mentioned in yeast cells reporting that DTT-induced expanded ER is degraded by autophagy (Bernales et al., 2006). Recently, ER-targeted autophagy named ER-phagy has been suggested to affect diverse physiological functions of ER such as protein synthesis and storage of calcium (Dikic, 2018). Four mammalian receptors for ER-phagy with different functions have been reported: FAM134B (Khaminets et al., 2015), RTN3 (Grumati et al., 2017), SEC62 (Fumagalli et al., 2016), and CCPG1 (Smith et al., 2018). Figure 4 shows the model for ER-phagy. The function of ER-phagy receptors are different; FAM134B and RTN3 participate in fragmentation of ER under starvation (Grumati et al., 2017; Khaminets et al., 2015). CCPG1 takes part in ER stress-induced ER-phagy, whereas SEC62 mediates ER clearance only during the recovery from ER stress (Fumagalli et al., 2016; Smith et al., 2018). Overall, the function of each ER-phagy receptors is diverse in circumstance (Chen et al., 2019) and the study about mechanism of ER-phagy has been improved. However, it is still insufficient which stimuli activate ER-phagy activity or what the physiological meaning of ER-phagy is. Although starvation is an important cue to induce ER-phagy, there is no single study of ER-phagy whereas general autophagy in the hypothalamus under starvation has been studied. Since starvation and diverse ER stress cues are known to induce ER-phagy, palmitate-induced ER stress might be involved in the regulation of ER-phagy. Given the starvation-induced ER stress (Henry et al., 2015) and autophagy (Coupé et al., 2021; Kaushik et al., 2011; Oh et al., 2016; Reginato et al., 2020) in hypothalamic cells, circulating palmitate under fasting might regulate ER stress and ER-phagy, affecting hypothalamic functions.

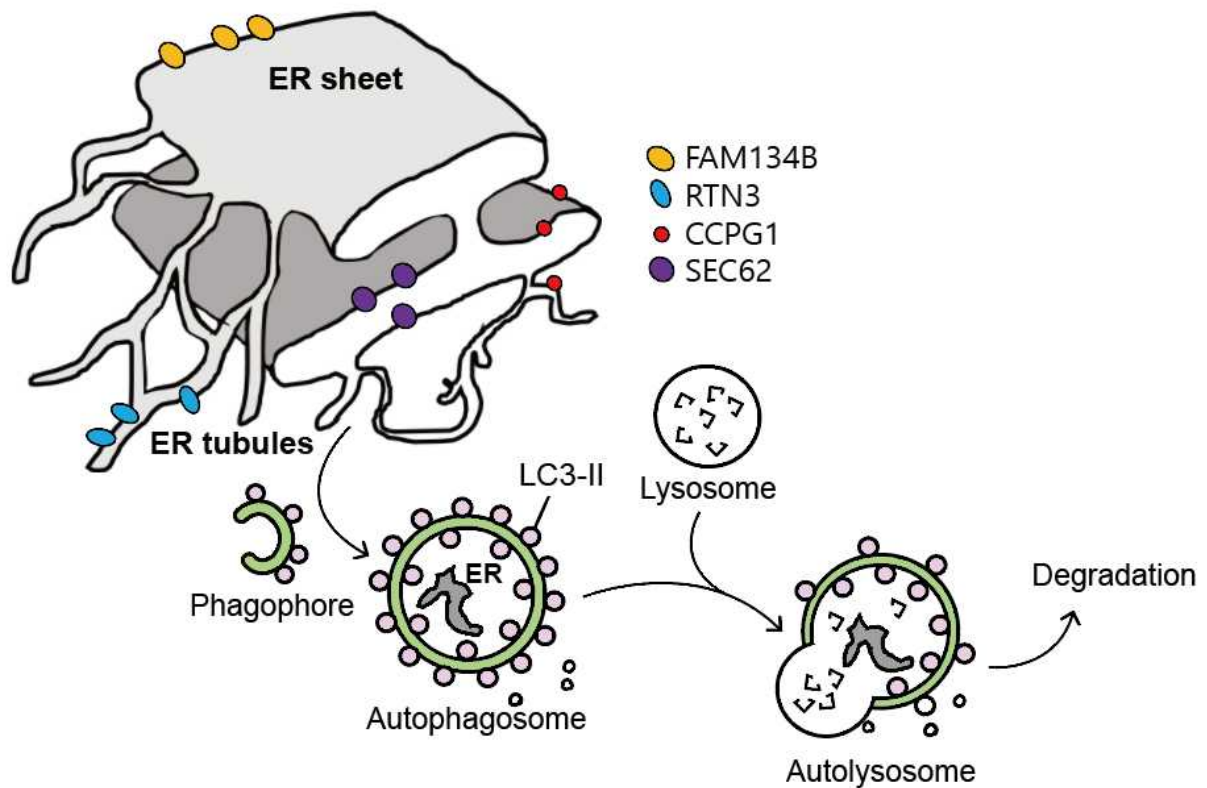


Figure 4. The model for ER-phagy. FAM134B, RTN3, CCPG1, and SEC62 are four major ER-phagy receptors. Depending on the stimulus, the ER-phagy receptor leads to the recruitment of autophagic membranes to initiate ER turnover. ER containing autophagosomes subsequently fuse with lysosomes.

5. Aims of the study

In this study, I sought to investigate the effect of palmitate on ER stress and ER-phagy in hypothalamic cells under starvation in comparison with nutrient-rich conditions. I demonstrated that palmitate increased ER stress and impaired ER-phagy by impeding autophagosome maturation under nutrient-rich conditions, but decreased ER stress and inhibited the initiation of ER-phagy under starvation. I discovered that ER-phagy is antecedent to ER stress and palmitate inhibits starvation-induced ER-phagy by increasing the expression of B-cell lymphoma 2 (Bcl-2). Thus, the blockade of ER-phagy by palmitate might alleviate the metabolic stress response under starvation. Taken together, I suggest a novel role of palmitate in suppressing starvation-induced hypothalamic stress by inhibiting ER-phagy and ER stress.

II. Materials and methods

1. Cell culture

N41 cells (mHypoE-N41, Cellutions Biosystems Inc., CLU121) were maintained in DMEM culture medium (Welgene, LM 001-07) supplemented with 10% fetal bovine serum (Corning, TCB101) and 1% penicillin/streptomycin (Hyclone Laboratories, SV30010) at 37 °C. Starvation was conducted by washing the cells twice with Earle's buffered salt solution (EBSS; Welgene, LB002-01) and then incubating them in fresh EBSS for 3 h.

2. Preparation of sodium palmitate

To prepare 100 mM palmitate solution, 27.8 mg of sodium palmitate (Sigma, P9767) was dissolved in 1 ml sterile water using a heating block at 70 °C for 10 min. Immediately after the incubation, 0.1 ml of 100 mM palmitate solution was added to 0.9 ml of serum-free DMEM containing 5% non-esterified fatty acid-free bovine serum albumin (Sigma, A9418), which was prepared at 40 °C, to produce 10 mM palmitate solution.

3. siRNA and plasmid transfection

ON-TARGETplus siRNAs for scrambled control (D-001810-10-20), mouse Bcl-2 (L-063933-00-0005), and mouse Fam134b (L-063361-01-0005) were purchased from Dharmacon. Cells were seeded in a 12-well plate for 24 h before transfection. Cells were transfected with siRNA (100 nM) using Lipofectamine 2000 (Invitrogen, 11668-019) according to the manufacturer's instructions. After 4 h, the medium was changed and the cells were incubated with a fresh medium for 48 h.

For plasmid transfection, cells were transfected with 1 μ g of plasmid using TurboFect Transfection Reagent (Thermo Fisher Scientific, R0534) according to the manufacturer's instructions. The plasmids were as follows: pmRFP-GFP encoding tandem-fluorescent LC3 (mRFP-GFP-LC3; a gift from Dr. Inhee Mook-Jung, Seoul National University); pmRFP-LC3 (Addgene, #21075); pDsRed2-Mito (Clontech, #632421); pEGFP-DFCP1 (Addgene, #38269); pEGFP-Parkin was generated by subcloning Myc-Parkin from pRK5-Myc-Parkin (Addgene, #17612; Ted Dawson's lab) into pEGFP-C1 (Clontech, #6084-1).

4. Immunocytochemistry

Cells were grown on coverslips coated with poly-L-lysine (Sigma, P4707), fixed in 10% formalin for 10 min and permeabilized with 0.1% saponin (Sigma, 47036) in PBS for 15 min. After washing with PBS, the coverslips were incubated with primary antibody diluted with antibody diluent solution (Invitrogen, #00-3118) for 1 h at room temperature (RT) and washed with PBS. Then, the coverslips were incubated with secondary antibody for 2 h at RT. After washing with PBS, the nuclei were stained for 10 min with Hoechst 33342 (Invitrogen, H3570) at a 1:3000 dilution in PBS. Finally, the coverslips were washed with PBS and mounted on microscope slides with ProLong Diamond Antifade Mountant (Thermo Fisher Scientific, P36970). Fluorescence images were examined under a confocal microscope (LSM 780 and LSM 800, Carl Zeiss) and analyzed in Zen software (Carl Zeiss).

5. Antibodies and reagents

Antibodies were purchased from the following sources: CCPG1 (ab219854) and KDEL (ab12223) were from Abcam; RTN3 (PA2256) was from Boster Biological Technology; ATF4 (#11815), ATF6 (#65880), Bcl-2 (#2870), Beclin1 (#3738), CHOP (#5554), COX IV (#4844),

GAPDH (#2118), IRE1 α (#3294), p-PERK (Thr980, #3179), and PERK (#3192) were from Cell Signaling Technology; FAM134B (NBP2-55248) and p-IRE1 α (Ser724, NB100-2323) were from Novus Biologicals; LC3 (L8918) and p62 (P0067) were from Sigma.

The secondary antibodies were purchased from the following sources: Goat anti-rabbit IgG (H+L) secondary antibody (31460) was from Thermo Fisher Scientific and Alexa488-conjugated anti-mouse (715–545-150) was from Jackson ImmunoResearch. Reagents were purchased from the following source: Bafilomycin A1 (B1793), carbonyl cyanide 3-chlorophenylhydrazone (CCCP; C2759), and sodium phenylbutyrate (4PBA; SML0309) were from Sigma.

6. Western blotting

Cells were lysed in buffer containing 50 mM Tris-HCl, pH 7.4, 250 mM sucrose (Bioshop, SUC507), 5 mM sodium pyrophosphate (Sigma, S6422), 1 mM EDTA (Sigma, E5134), 1 mM EGTA (Sigma, E3889), 1% Triton X-100 (Sigma, T8787), 0.1 mM benzamidine (Sigma, B6506), 1 mM dithiothreitol (Sigma, #43816), 0.5 mM phenylmethylsulfonyl fluoride (Sigma, P7626), 50 mM sodium fluoride (Sigma, 201154), protease inhibitor cocktail (Calbiochem, #535140), and phosphatase inhibitor cocktail (Sigma, P5726). After 30 min of incubation on ice, lysates were centrifuged at 16,400 \times g for 15 min and protein concentration in the supernatants was measured using a Pierce BCA protein assay kit (Thermo Fisher Scientific, #23225). Total protein (7 μ g) was loaded on a SDS-polyacrylamide gel and blotted onto PVDF membranes (Millipore, IPVH00010) for 35 min at 20 V/cm in transfer buffer containing 25 mM Tris, 192 mM glycine, and 20% methanol. The membrane was blocked by 1 h incubation with 5% skim milk. After blocking, the membrane was incubated with the specific primary antibody for 1 h at RT or overnight at 4 $^{\circ}$ C. After three washes with 1 \times TBST buffer containing 20 mM Tris, 125 mM NaCl, 0.1% Tween 20 (Sigma, P1379), pH 7.4, the membrane was incubated with secondary antibody and visualized by using ECL solutions (Thermo Fisher Scien-

tific, #34580 and #34095) according to the recommended procedure. SRX 201A (Konica Minolta Medical Imaging) was used to develop films. Obtained images were analyzed using Image J software (National Institutes of Health) and the level of each protein was quantified and normalized to that of GAPDH.

7. RNA extraction and quantitative Real time PCR

Total RNA from the N41 cells was extracted with TRIzol reagent (Invitrogen, #15596018), and its concentration was determined using a NanoDrop spectrophotometer (Thermo Scientific). RNA (3 μ g) was reverse transcribed using a GoScript Reverse Transcription System (Promega, A5004) as described previously (B'Chir et al.). TB Green (TaKaRa Biotechnology, RR820A) was used for quantitative PCR estimation of the expression of *Beclin1* and *Gapdh* genes in a CFX 96 Real-Time system (Bio-Rad). Sequences of primers used in qRT-PCR are listed in Table 1. The expression level was normalized to that of *Gapdh* as an endogenous control. All assays were performed in triplicate.

8. Statistical analysis

Data from at least three independent experiments were expressed as the mean \pm standard error of the mean (SEM). Statistical significance was determined using one-way analysis of variance followed by Tukey's multiple comparisons test using GraphPad Prism 8.0.1 (GraphPad Software).

Table 1. Sequences of primers used for qRT-PCR

<i>Gene name</i>	Accession No.		Primer sequence	Product size
<i>Beclin1</i>	NM_019584.4	forward	5'-GGCGGCTCCTATTCCATC-3'	108 bp
		reverse	5'-TGAGGACACCCAAGCAAG-3'	
<i>Gapdh</i>	NM_001289726.1	forward	5'-ATCACTGCCACCCAGAAGAC-3'	181 bp
		reverse	5'-ACACATTGGGGGTAGGAACA-3'	

III. Results

1. Palmitate induces ER stress

To examine the effect of palmitate on ER stress in the mouse hypothalamic cell line N41 under normal nutrient-rich conditions, I checked the activation of three UPR sensor proteins, IRE1, PERK, and ATF6, following treatment with various concentrations of palmitate (Fig. 5a, b). Palmitate treatment for 12 h increased the levels of both p-PERK (50 and 100 μ M) and ATF6 (100 μ M), while p-IRE1 did not change (Fig. 5a, b). Also, the levels of ATF4 and CHOP, the late ER stress markers (Fusakio et al., 2016), were increased after 12 h treatment with palmitate (50 and 100 μ M). The increases in the levels of p-PERK, ATF6, ATF4, and CHOP by palmitate at 24 h were less robust compared with 12 h treatment.

Since the levels of ER stress markers were highest at 12 h with 100 μ M of palmitate, the effect of this concentration was tested at three different early time points (Fig. 6a, b). While PERK was gradually phosphorylated, the level of ATF6 increased only at 12 h and the level of p-IRE1 did not change (Fig. 6a, b). A significant elevation in the levels of ATF4 and CHOP (Fig. 6a, b) suggests that the p-PERK–ATF4–CHOP axis is the major ER stress pathway activated by palmitate in N41 cells.

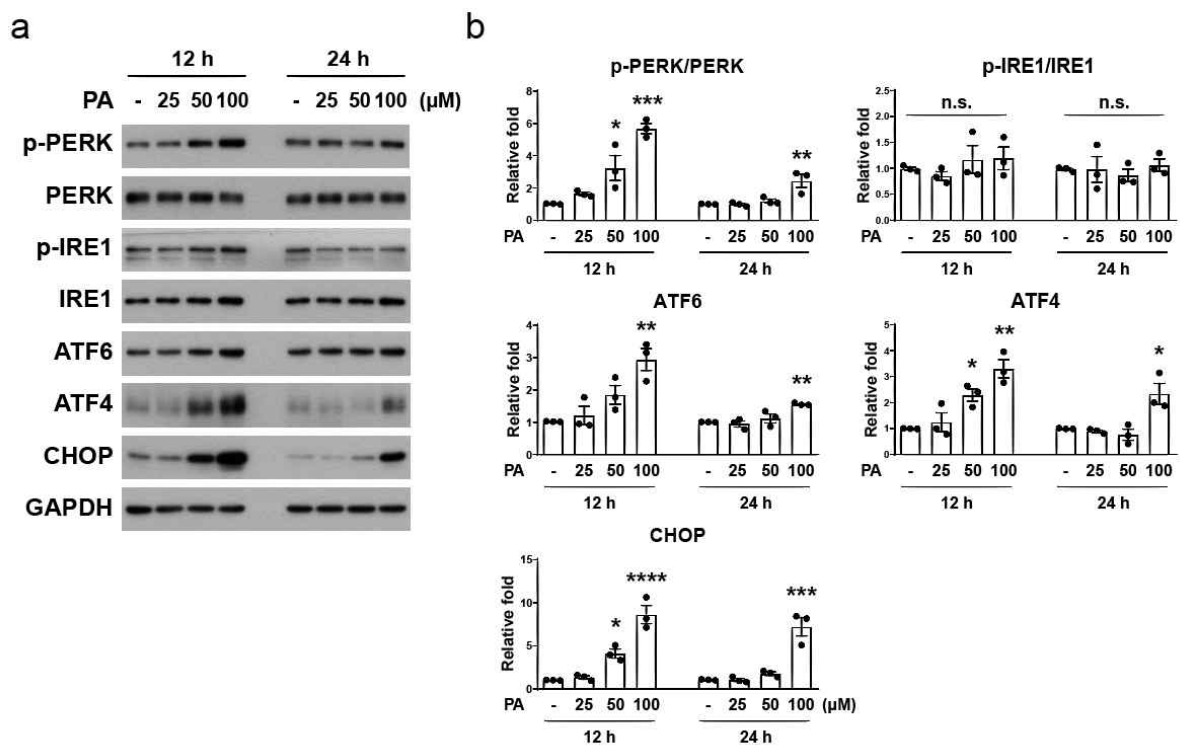


Figure 5. The effect of palmitate on ER stress in different time points and doses in hypothalamic N41 cells. Immunoblotting analysis (a) and quantification (b) of ER stress markers (p-PERK, PERK, p-IRE1, IRE1, ATF6, ATF4, and CHOP) in cells treated with different concentrations of palmitate (25, 50, and 100 μ M) for the indicated times ($n = 3$ per each group). Data are mean \pm SEM; p-PERK/PERK; * $p=0.0252$, *** $p=0.0003$ vs. control at 12 h, ** $p=0.0065$ vs. control at 24 h, ATF6; ** $p=0.0040$ vs. control at 12 h, ** $p=0.0074$ vs. control at 24 h, ATF4; * $p=0.0454$, ** $p=0.0017$ vs. control at 12 h, * $p=0.00139$ vs. control at 24 h, CHOP; * $p=0.0240$, **** $p<0.0001$ vs. control at 12 h, *** $p=0.0002$ vs. control at 24 h. n.s., no significant difference.

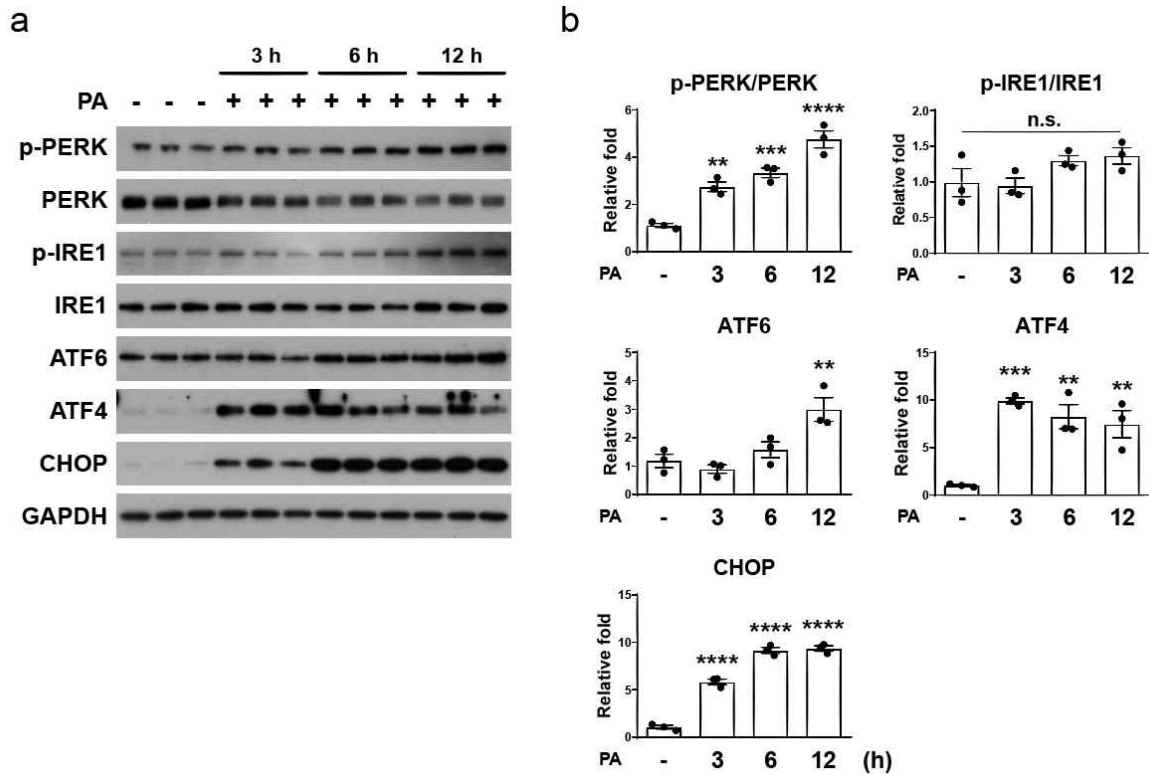


Figure 6. Palmitate induces ER stress in N41 cells. Immunoblotting analysis (a) and quantification (b) of ER stress markers in cells treated with 0.1 mM palmitate for the indicated times (n = 3 per each group). Data are mean \pm SEM; p-PERK/PERK; ** $p=0.0050$, *** $p=0.0007$, **** $p<0.0001$ vs. control, ATF6; ** $p=0.0091$ vs. control, ATF4; ** $p=0.0033$ at PA 6 h vs. control, ** $p=0.0067$ at PA 12 h vs. control, *** $p=0.0009$ vs. control, CHOP; **** $p<0.0001$ vs. control. n.s., no significant difference.

2. Palmitate induces autophagy in a short time treatment but the prolonged treatment of palmitate impairs autophagy

Since ER stress regulates autophagy (B'Chir et al., 2013), I assessed the effect of palmitate on autophagy in N41 cells. I used the levels of LC3 and p62 as readouts for autophagy induction. When autophagy is induced, the LC3-I form is converted to LC3-II through lipidation (Tanida et al., 2004). At the same time, p62, a receptor protein that brings the cargo to the phagophore, is degraded (Bjorkoy et al., 2009). To further monitor the autophagy flux induced by palmitate, I used bafilomycin A1 (Baf A1), a pharmacological inhibitor of autophagy (Klionsky et al., 2016). Baf A1 blocks the fusion of autophagosomes with lysosomes, impairing autophagy flux and cargo degradation (Klionsky et al., 2016). Therefore, the more accumulation of p62 and LC3-II after Baf A1 treatment indicates accumulated autophagosomes due to increased autophagy flux. Baf A1 co-treatment increased the levels of both p62 and LC3-II in comparison with palmitate alone only at 3 h but not at 6 h or 12 h, suggesting that palmitate induced autophagy flux at 3 h but impaired autophagy at 6 h and 12 h (Fig. 7a, b).

To further confirm autophagy status, mRFP-GFP-LC3 fluorescence puncta assay was used. In the mRFP-GFP-LC3 fluorescent puncta assay, mRFP-GFP-LC3 puncta display both green and red fluorescence in autophagosome while display red only in autolysosome. The RFP signal is more stable than GFP in acidic conditions, so the GFP signal is degraded in autolysosome. Depending on the different colors, the autophagy flux can be estimated by counting yellow puncta (autophagosomes) and red puncta (autolysosomes) (Kimura et al., 2007). In addition, the analysis of the puncta number ratio of yellow to red is useful to estimate the transition from autophagosome to autolysosome. In N41 cells expressing mRFP-GFP-LC3, palmitate increased the total number of red plus yellow puncta at all time points (Fig. 7c, d). However, based on a significantly higher ratio of yellow puncta over red, the increases in total puncta at 6 h and 12 h are not due to increased autophagy influx but rather, to the accumulation of autophagosomes of which degradation is impaired (Fig. 7c, d). These data suggest

that prolonged treatments with palmitate such as 6 h and 12 h impaired autophagy by undermining autophagosome–lysosome fusion and autophagosome degradation. Also, considering that there are no increases in p62 and LC3-II at 6 h and 12 h after Baf A1 treatment with palmitate, palmitate impaired autophagy at 6 h and 12 h. Collectively, these results show that palmitate induces ER stress and autophagy at 3 h but impairs autophagy at 6 h and 12 h.

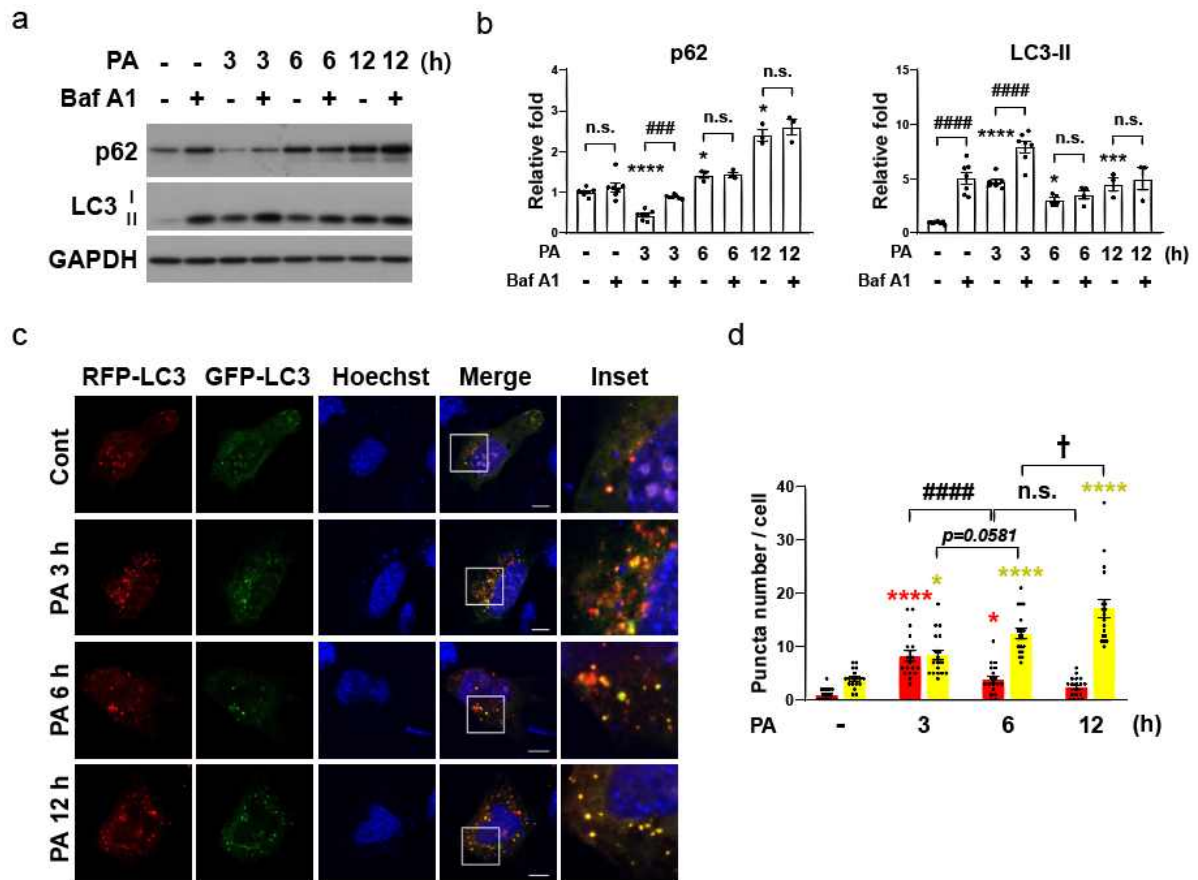


Figure 7. Palmitate induces autophagy at early time points, but prolonged treatment of palmitate impairs autophagy in N41 cells. **a** and **b** Immunoblotting analysis (**a**) and quantification (**b**) of autophagy markers (p62 and LC3-II) in cells treated with 0.1 mM palmitate for the indicated times. Baf A1 (200 nM) was added for 3 h before harvest (p62; $n = 7$ for control, control + Baf A1, PA 3 h, PA 3 h + Baf A1, $n = 3$ for PA 6 h, PA 6 h + Baf A1, PA 12 h, PA 12 h + Baf A1, LC3-II; $n = 8$ for control, $n = 7$ for control + Baf A1, PA 3 h, PA 3 h + Baf A1, $n = 4$ for PA 6 h, PA 6 h + Baf A1, $n = 3$ for PA 12 h, PA 12 h + Baf A1. Data are mean \pm SEM; p62; $*p=0.0295$ at PA 6 h vs. control, $*p=0.0250$ at 12 h vs. control, $****p<0.0001$ vs. control, $####p=0.0008$, LC3-II; $*p=0.0444$, $****p=0.0003$, $****p<0.0001$ vs. control, $#####p<0.0001$. **c** and **d** Cells transiently expressing mRFP-GFP-LC3 were treated with 0.1 mM palmitate for the indicated times. Representative micrographs (**c**) and quantification (**d**) of the average number of mRFP-GFP-LC3 puncta per cell ($n = 18$ per each group). Scale bar, 10 μ m. Data are mean \pm SEM; Red puncta; $*p=0.0158$, $****p<0.0001$ vs. control, $#####p<0.0001$, Yellow puncta; $*p=0.0257$, $****p<0.0001$ vs. control, $^\dagger p=0.0174$. n.s., no significant difference.

3. Palmitate impairs ER-phagy at the autophagosome maturation step

ER stress induced by the accumulation of unfolded proteins may drive ER-phagy to maintain ER proteostasis (Smith et al., 2018). To examine whether palmitate-induced ER stress triggers ER-phagy in N41 cells, I measured the proteolytic degradation of ER-phagy receptors FAM134B, RTN3, and CCPG1 as the markers of ER-phagy (Grumati et al., 2017; Khaminets et al., 2015; Smith et al., 2018) after palmitate treatment (Fig. 8a, b). Palmitate treatment for 6 h or 12 h increased the levels of FAM134B and CCPG1 but had no effect on the RTN3 level (Fig. 8a, b). Because autophagy was impaired after 6 h and 12 h palmitate treatment (Fig. 7a–d), the elevated FAM134B and CCPG1 levels suggested the impairment of ER-phagy.

To visualize ER-phagy and distinguish ER-containing autophagosomes and autolysosomes in palmitate-treated cells, I analyzed the colocalization of mRFP-LC3 and KDEL (ER marker) in the presence or absence of Baf A1 (Fig. 9a). Colocalization was increased by Baf A1 in the absence of palmitate, showing ER-phagy at basal state (Fig. 9a, b). However, despite the overall increase in colocalization at 6 h and 12 h, its level was not affected by Baf A1, indicating stalled ER-phagy at autophagosomes at these time points (Fig. 9a, b).

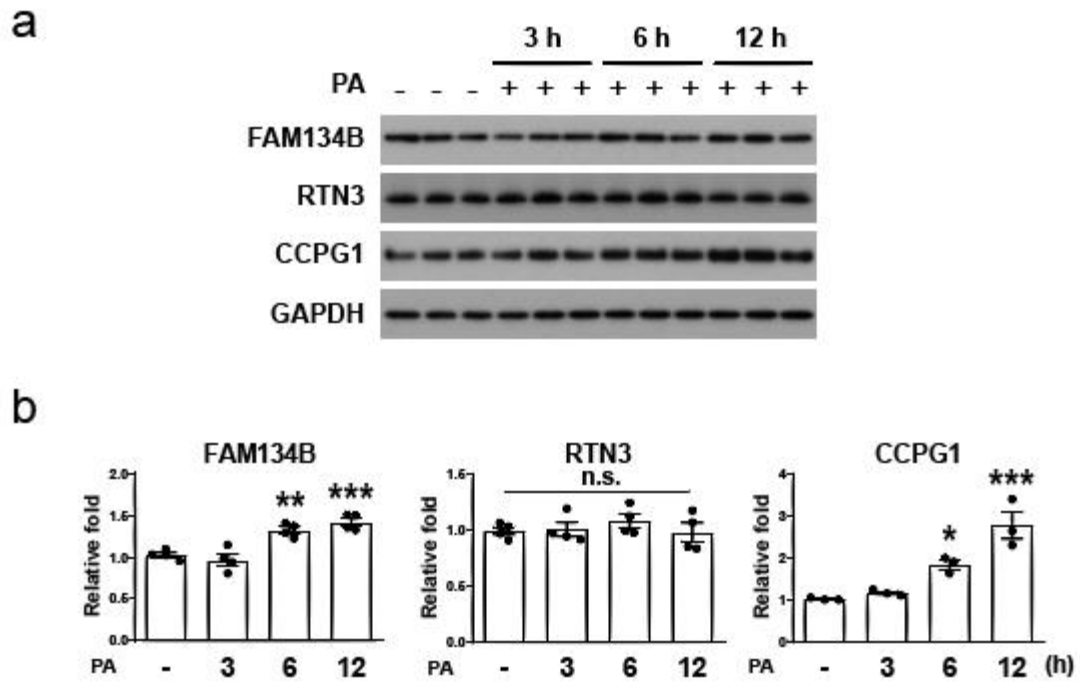


Figure 8. The effect of palmitate on ER-phagy receptors in N41 cells. Immunoblotting analysis (a) and quantification (b) of ER-phagy receptors (FAM134B, RTN3, and CCPG1) in cells treated with 0.1 mM palmitate for the indicated times (FAM134B and RTN3; n = 4 per each group, CCPG1; n = 3 per each group). Data are mean \pm SEM; FAM134B; ** $p=0.0053$, *** $p=0.0005$ vs. control, CCPG1; * $p=0.0388$, *** $p=0.0004$ vs. control. n.s., no significant difference.

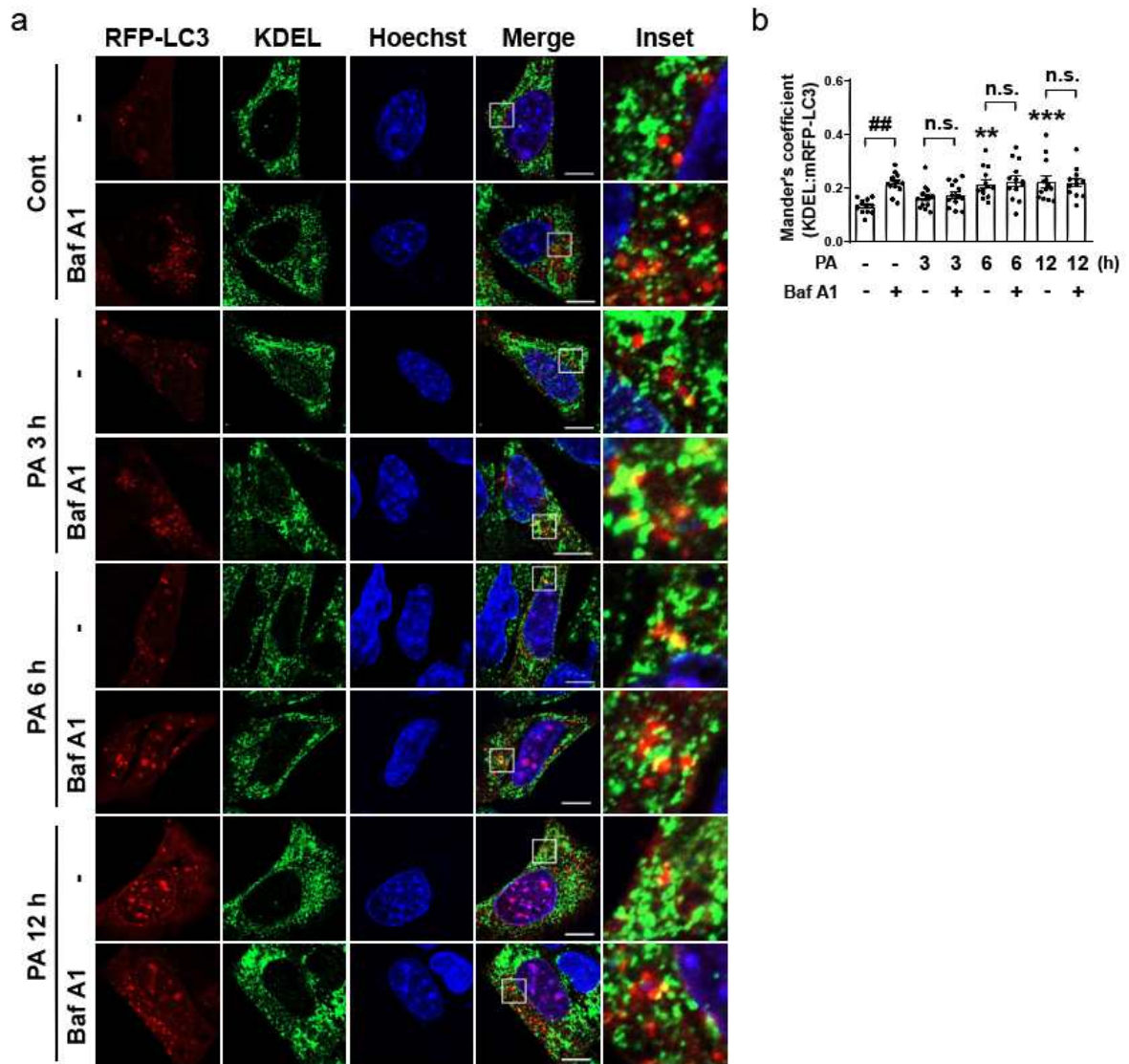


Figure 9. Palmitate impairs ER-phagy in N41 cells. Cells transiently expressing mRFP-LC3 were treated with 0.1 mM palmitate for the indicated times in the presence or absence of Baf A1 (200 nM). Treated cells were stained for the ER marker KDEL. Representative micrographs (**a**) and quantification (**b**) of colocalization between mRFP-LC3 and KDEL ($n = 13$ per each group). Scale bar, 10 μ m. Data are mean \pm SEM; ** $p=0.0029$, *** $p=0.0008$ vs. control, ## $p=0.0025$. n.s., no significant difference.

4. Palmitate does not induce mitophagy

Palmitate might also regulate mitophagy, selective autophagy that degrades damaged mitochondria (Chen et al., 2018; Wu et al., 2015). To investigate whether palmitate induces mitophagy, I monitored selective translocation of Parkin (E3 ubiquitin ligase) from the cytosol to dysfunctional mitochondria, the well-known pathway of mitophagy (Narendra et al., 2008). The recruitment of Parkin to mitochondria was visualized by exogenous expression of GFP-Parkin and DsRed2-Mito (Fig. 10a, b). While the treatment with the mitophagy-inducing protonophore CCCP showed clear recruitment of Parkin to mitochondria, there was no mitochondrial translocation of Parkin in palmitate-treated cells at any time point (Fig. 10a, b).

Consistently, the protein level of cytochrome *c* oxidase subunit 4 isoform 1 (COX IV), one of the mitochondrial marker proteins, was not changed by palmitate, but was significantly decreased by CCCP treatment (Fig. 11a, b). Taken together, these results indicate that palmitate selectively impairs ER-phagy and does not affect mitophagy in N41 cells under nutrient-rich conditions.

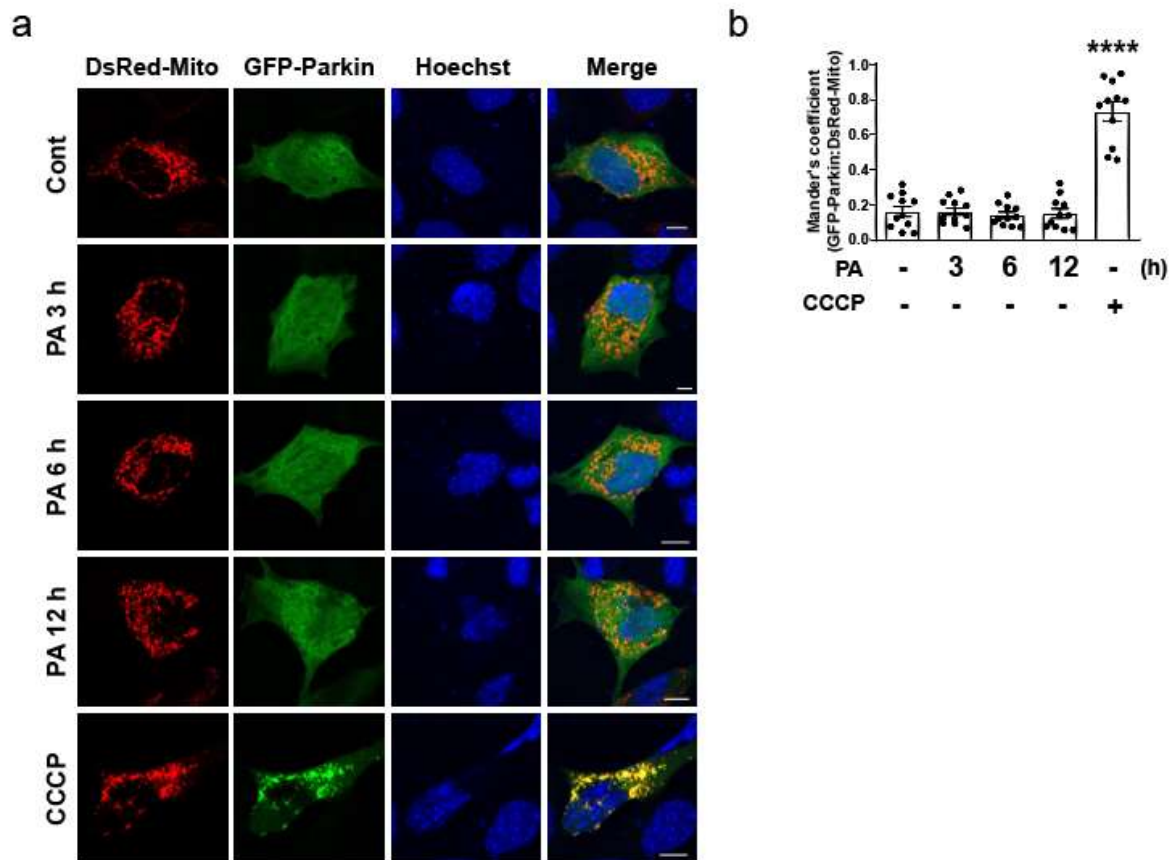
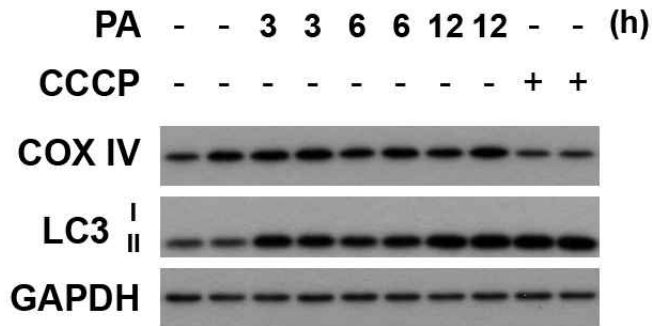


Figure 10. Palmitate does not induce recruitment of parkin to mitochondria in N41 cells. Cells were treated with 0.1 mM palmitate for the indicated times. CCCP (50 μ M) was added for 3 h as the positive control for mitophagy. **a** and **b** Cells transiently expressing DsRed-Mito and GFP-Parkin were treated with 0.1 mM palmitate for the indicated times. Representative micrographs (**a**) and quantification (**b**) of colocalization between DsRed-Mito and GFP-Parkin (n = 11 per each group). Scale bar, 10 μ m. Data are mean \pm SEM; **** p < 0.0001 vs. control.

a



b

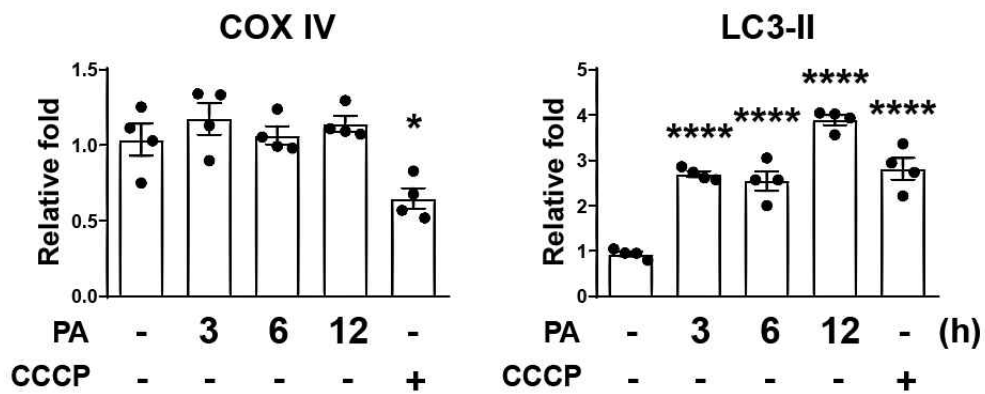


Figure 11. Palmitate does not accumulate COX IV in N41 cells. Cells were treated with 0.1 mM palmitate for the indicated times. CCCP (50 μ M) was added for 3 h as the positive control for mitophagy. Immunoblotting analysis (a) and quantification (b) of the mitochondrial marker COX IV and LC3-II (n = 4 per each group). Data are mean \pm SEM; COX IV; * $p=0.0291$ vs. control, LC3-II; **** $p<0.0001$ vs. control.

5. Short-term treatment with palmitate inhibits ER-phagy under starvation

Since ER-phagy was impaired by prolonged palmitate treatment (≥ 6 h) under nutrient-rich conditions, I further examined whether palmitate also inhibits starvation-induced ER-phagy. ER-phagy is highly upregulated in response to nutrient deprivation such as nitrogen starvation (Nakatogawa, 2016) and EBSS (Smith et al., 2018). The incubation of hypothalamic cells in EBSS for 3 h significantly increased the colocalization of mRFP-LC3 and KDEL, and the treatment with Baf A1 further increased the colocalization due to the blockage of KDEL-containing proteins degradation and their accumulation in autophagosomes (Fig. 12a, b). Interestingly, the treatment of starved cells with palmitate for 3 h, the time point at which palmitate did not impair autophagy under nutrient-rich conditions, greatly reduced the colocalization (Fig. 12a, b). Since Baf A1 had no additional effect on this reduction, palmitate might block an early stage of the autophagic process such as autophagosome formation, rather than degradation of ER compartments.

To determine the difference in the proportion of ER-phagy in the overall autophagic process induced by EBSS and/or palmitate, I analyzed the ratio of the number of KDEL-positive mRFP-LC3 puncta to total mRFP-LC3 puncta (Fig. 12c). Whereas the ratio of ER-phagy after palmitate treatment (17%) was similar to that in basal state (11%) or additional Baf A1 treatment (20%), EBSS-induced ER-phagy accounted for about 50% of total autophagy and its ratio was dramatically decreased by palmitate (15%) similar to the basal ER-phagy ratio, implying that palmitate almost completely inhibits ER-phagy induced by EBSS.

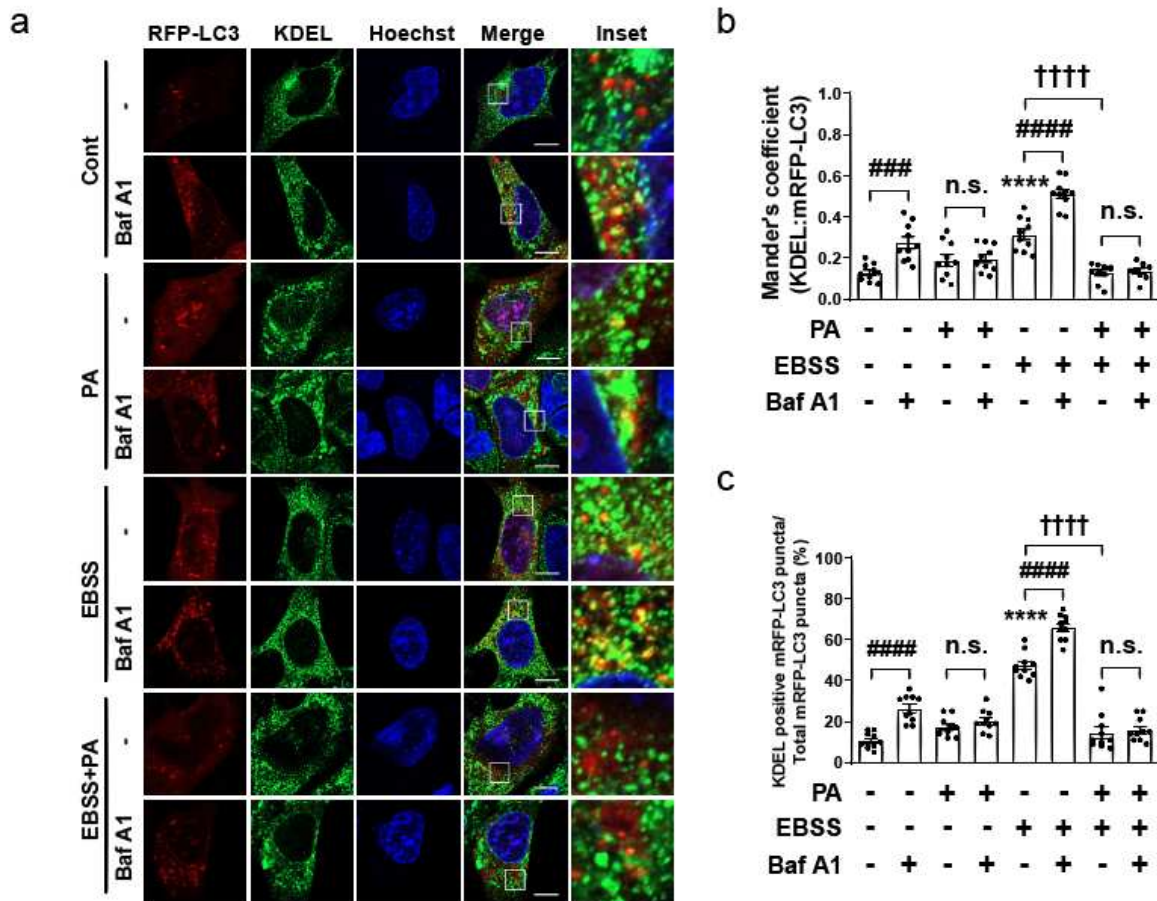


Figure 12. Palmitate inhibits EBSS-induced colocalization of mRFP-LC3 and KDEL in N41 cells. Cells transiently expressing mRFP-LC3 were starved in EBSS for 3 h in the presence or absence of palmitate (0.1 mM) and were co-treated for 3 h with Baf A1. Treated cells were stained for the ER marker KDEL. Representative micrographs (**a**) and quantification (**b**) of colocalization between mRFP-LC3 and KDEL (n = 10 per each group). Scale bar, 10 μ m. Data are mean \pm SEM; **** $p < 0.0001$ vs. control, ### $p = 0.0002$, ##### $p < 0.0001$, ††† $p < 0.0001$. **c** The ratio of the average number of KDEL-positive mRFP-LC3 puncta to the total number of mRFP-LC3 puncta per cell (n = 10 per each group). Data are mean \pm SEM; **** $p < 0.0001$ vs. control, ##### $p < 0.0001$, ††† $p < 0.0001$. n.s., no significant difference.

Next, I assessed which ER-phagy cargo receptors are involved in the inhibition of ER-phagy by palmitate under starvation (Fig. 13a, b). EBSS significantly decreased the levels of both FAM134B and CCPG1, whereas additional treatment with palmitate or Baf 1A increased the level of FAM134B only. The level of LC3-II was also decreased by EBSS due to rapid degradation, evident from the accumulation of the protein in cells treated with palmitate or Baf A1 under starvation. While treatment of Baf A1 with EBSS significantly increased FAM134B compared to EBSS only, the treatment of Baf A1 with palmitate plus EBSS did not change FAM134B compared to palmitate plus EBSS, suggesting that palmitate inhibits the degradation of FAM134B under starvation. However, the level of RTN3 was not changed by EBSS, palmitate, or Baf A1. Taken together, these data suggest that, unlike under nutrient-rich conditions, palmitate treatment for 3 h inhibits EBSS-induced ER-phagy, which is mediated, at least in part, by FAM134B.

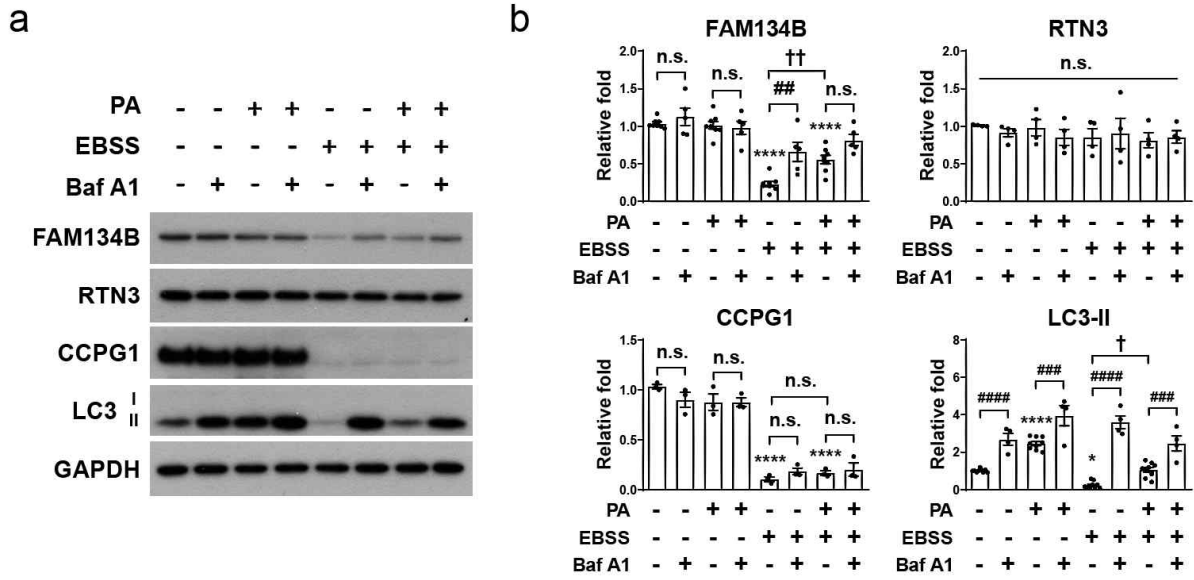


Figure 13. Palmitate blocks EBSS-induced ER-phagy in N41 cells. Immunoblotting analysis (a) and quantification (b) of ER-phagy receptors and LC3-II in cells starved in EBSS for 3 h in the presence or absence of palmitate (0.1 mM) and were co-treated for 3 h with Baf A1 (FAM134B; n = 8 for control, PA, EBSS, PA + EBSS, n = 5 for control + Baf A1, PA + Baf A1, EBSS + Baf A1, PA + EBSS + Baf A1, RTN3; n = 4 per each group, CCPG1; n = 3 per each group, LC3-II; n = 9 for control, PA, EBSS, PA + EBSS, n = 4 for control + Baf A1, PA + Baf A1, EBSS + Baf A1, PA + EBSS + Baf A1). Data are mean \pm SEM; FAM134B; **** $p < 0.0001$ vs. control, ## $p = 0.0016$, †† $p = 0.0094$, CCPG1; **** $p < 0.0001$ vs. control, LC3-II; * $p = 0.0331$, **** $p < 0.0001$ vs. control, #### $p = 0.0002$ at PA vs. PA + Baf A1, #### $p = 0.0005$ at PA + EBSS vs. PA + EBSS + Baf A1, ##### $p < 0.0001$, † $p = 0.0203$. n.s., no significant difference.

6. ER-phagy precedes ER stress and palmitate reduces ER stress by inhibiting ER-phagy under starvation

Next, I examined whether palmitate regulates starvation-induced ER stress. Starvation increased the levels of ATF4 and CHOP, but decreased those of the upstream UPR sensor proteins such as p-PERK, p-IRE1, and ATF6 (Fig. 14a, b), suggesting that EBSS induces ER stress independently of the three UPR sensors (Shin et al., 2015). Interestingly, the levels of ATF4 and CHOP increased by EBSS were greatly diminished by palmitate (Fig. 14a, b). Thus, these results demonstrate that palmitate reduces starvation-induced ER stress.

To investigate the relationship between ER-phagy and ER stress under starvation, both of which are inhibited by palmitate, I inhibited ER stress and ER-phagy by 4PBA pretreatment and by knockdown of *Fam134b*, respectively, and then examined the markers of ER-phagy and ER stress in cells treated with EBSS and/or palmitate (Fig. 15a–d). The colocalization of mRFP-LC3 and KDEL was significantly reduced by *Fam134b* knockdown under EBSS conditions, but no change was observed in 4PBA pretreatment, suggesting that ER-phagy was not affected by ER stress under starvation (Fig. 15a, b). The inhibition of the colocalization of ER and autophagosomes by palmitate was maintained in both 4PBA pretreatment and *Fam134b* knockdown under starvation (Fig. 15a, b), consistent with palmitate-induced accumulation of FAM134B in 4PBA pretreatment under starvation (Fig. 5c, d). However, *Fam134b* knockdown did not lead to any accumulation of FAM134B induced by palmitate under starvation (Fig. 5c, d). Thus, these results indicate that palmitate inhibits ER-phagy in an ER stress- and *Fam134b*-independent manner. On the contrary, the level of CHOP was significantly decreased by *Fam134b* knockdown under starvation, demonstrating that ER-phagy precedes and is required for ER stress under starvation. Decreased level of CHOP by palmitate under EBSS in *Fam134b*-knockdown cells compared to that of EBSS conditions in *Fam134b*-knockdown cells might be due to sustained inhibition of ER-phagy by palmitate (Fig 4c, d). Therefore, palmitate reduces ER stress by inhibiting ER-phagy under starvation.

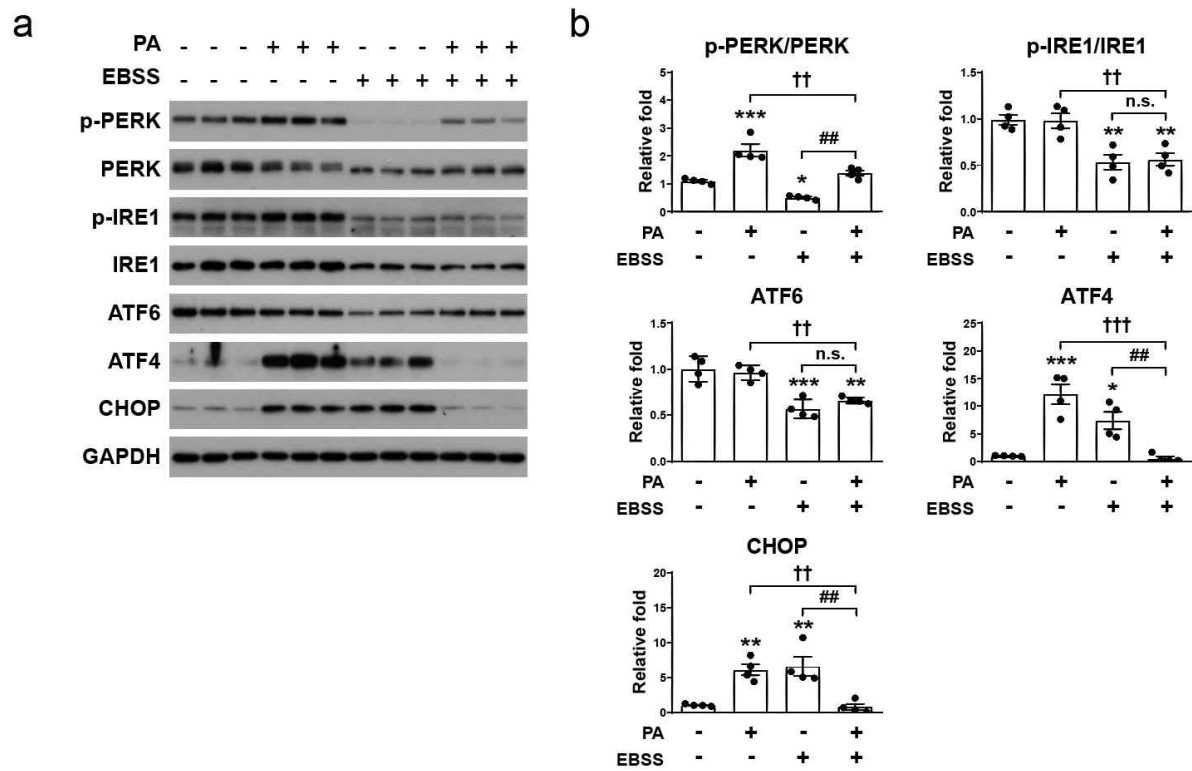


Figure 14. Palmitate inhibits EBSS-induced ER stress in N41 cells. Cells were starved in EBSS for 3 h in the presence or absence of palmitate (0.1 mM). Immunoblotting analysis (**a**) and quantification (**b**) of ER stress markers in cells starved in EBSS for 3 h in the presence or absence of palmitate ($n = 4$ per each group). Data are mean \pm SEM; p-PERK/PERK; $*p=0.0220$, $***p=0.0002$ vs. control, $##p=0.0012$, $††p=0.0021$, p-IRE1/IRE1; $**p=0.0038$ at EBSS vs. control, $**p=0.0060$ at PA + EBSS vs. control, $††p=0.0072$, ATF6; $**p=0.0012$, $***p=0.0001$ vs. control, $††p=0.0032$, ATF4; $*p=0.0146$, $***p=0.0002$ vs. control, $##p=0.0094$, $†††p=0.0001$, CHOP; $**p=0.0045$ at PA vs. control, $**p=0.0022$ at EBSS vs. control, $##p=0.0016$, $††p=0.0032$.

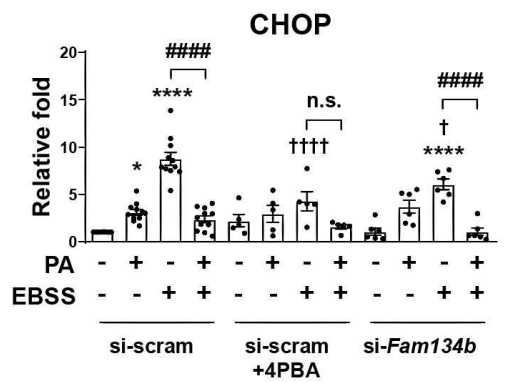
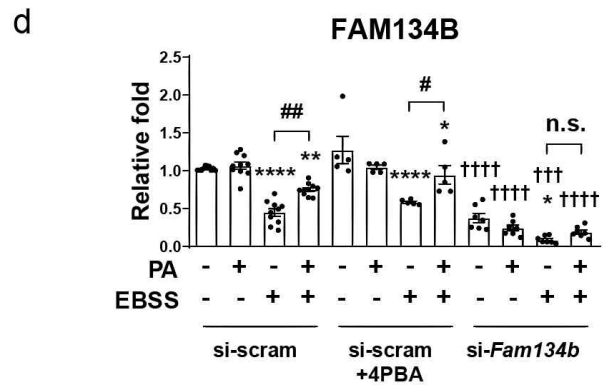
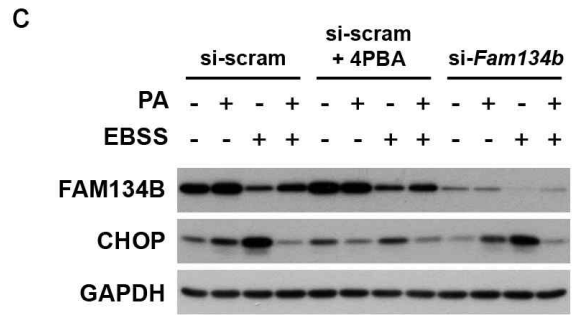
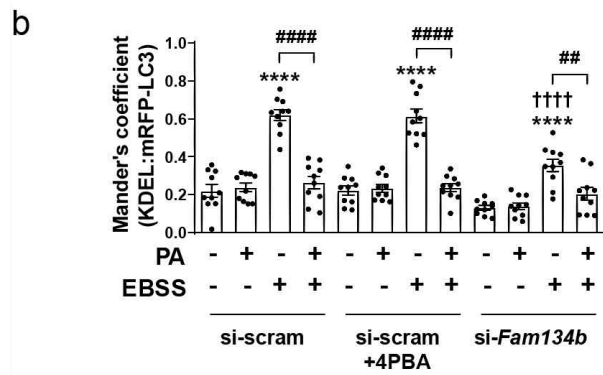
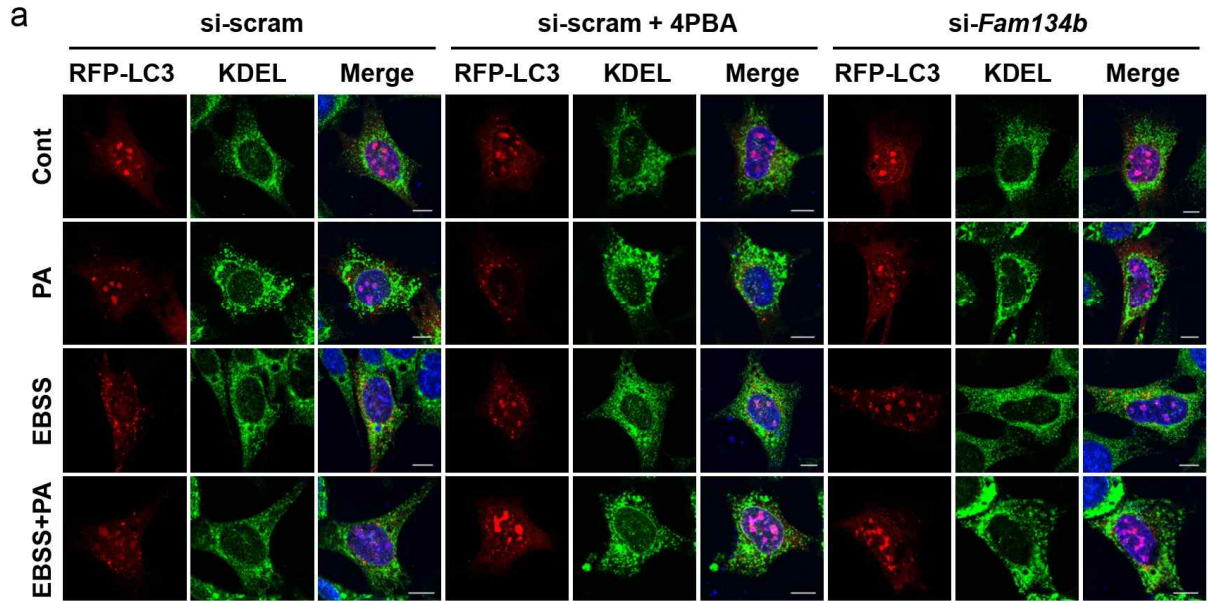


Figure 15. Inhibitory effect of palmitate on EBSS-induced ER-phagy precedes EBSS-induced ER stress in N41 cells. **a** and **b** Cells transfected with mRFP-LC3 24 h after transfection with si-scram or si-*Fam134b* were starved in EBSS for 3 h in the presence or absence of palmitate (0.1 mM). Cells transfected with si-scram were pretreated with 4PBA (5 mM) for 1 h before starvation. After all treatments, cells were stained for the ER marker KDEL. Representative micrographs (**a**) and quantification (**b**) of colocalization between mRFP-LC3 and KDEL (n = 10 per each group). Scale bar, 10 μ m. Data are mean \pm SEM; **** $p < 0.0001$ vs. each control in si-scram, si-scram + 4PBA, si-*Fam134b*, ## $p = 0.0097$, #### $p < 0.0001$, ††† $p < 0.0001$ vs. EBSS in si-scram. **c** and **d** Cells transfected with si-scram or si-*Fam134b* were starved in EBSS for 3 h in the presence or absence of palmitate (0.1 mM). Cells transfected with si-scram were pretreated with 4PBA (5 mM) for 1 h before starvation. Immunoblotting analysis (**c**) and quantification (**d**) of FAM134B and CHOP (FAM134B; n = 10 for si-scram, n = 5 for si-scram + 4PBA, n = 7 for si-*Fam134b* group, CHOP; n = 11 for si-scram, n = 5 for si-scram + 4PBA, n = 6 for si-*Fam134b* group). Data are mean \pm SEM; FAM134B; ** $p = 0.0051$ at PA + EBSS in si-scram vs. control in si-scram, **** $p < 0.0001$ at EBSS in si-scram vs. control in si-scram, * $p = 0.0419$ at PA + EBSS in si-scram + 4PBA vs. control in si-scram + 4PBA, **** $p < 0.0001$ at EBSS in si-scram + 4PBA vs. control in si-scram + 4PBA, * $p = 0.0295$ at EBSS in si-*Fam134b* vs. control in si-*Fam134b*, # $p = 0.0139$, ## $p = 0.0013$, ††† $p = 0.0004$ at EBSS in si-*Fam134b* vs. EBSS in si-scram, †††† $p < 0.0001$ vs. each control, PA, PA + EBSS in si-scram, CHOP; * $p = 0.0372$ vs. control in si-scram, **** $p < 0.0001$ at EBSS in si-scram vs. control in si-scram, **** $p < 0.0001$ at EBSS in si-*Fam134b* vs. control in si-*Fam134b*, #### $p < 0.0001$, † $p = 0.0170$ vs. control in si-scram, †††† $p < 0.0001$ vs. control in si-scram. n.s., no significant difference.

7. Palmitate inhibits ER-phagy at the initiation step by increasing Bcl-2 level under starvation

Next, I investigated how palmitate prevents ER-phagy under starvation. I counted the number of mRFP-LC3 puncta, which represent autophagosomal compartments (Yoshii and Mizushima, 2017), in cells treated with EBSS and/or palmitate treatment (Fig. 16a, b). Each treatment increased the number of mRFP-LC3 puncta, whereas combined treatment decreased it to a level similar to that of control, suggesting that palmitate decreased autophagy under starvation. I also performed the experiments using double FYVE-domain-containing protein 1 (DFCP1), an early autophagy marker (Axe et al., 2008b), to check the initiation of autophagosome formation (Fig. 17a, b). Similar to the result of mRFP-LC3 puncta, the number of GFP-DFCP1 puncta was decreased in co-treatment with palmitate and EBSS while that was increased by either palmitate or EBSS, confirming that palmitate decreased autophagosome formation under starvation.

The ATG proteins are necessary for the biogenesis of autophagosomes. Although it was reported that palmitate inhibits autophagy by degrading ATG5 (Mallik and Yammani, 2018) or decreasing the expression of ATG7 (Nissar et al., 2017), the protein levels of ATG5 and ATG7 were not changed by palmitate treatment under starvation (Fig. 18a, b).

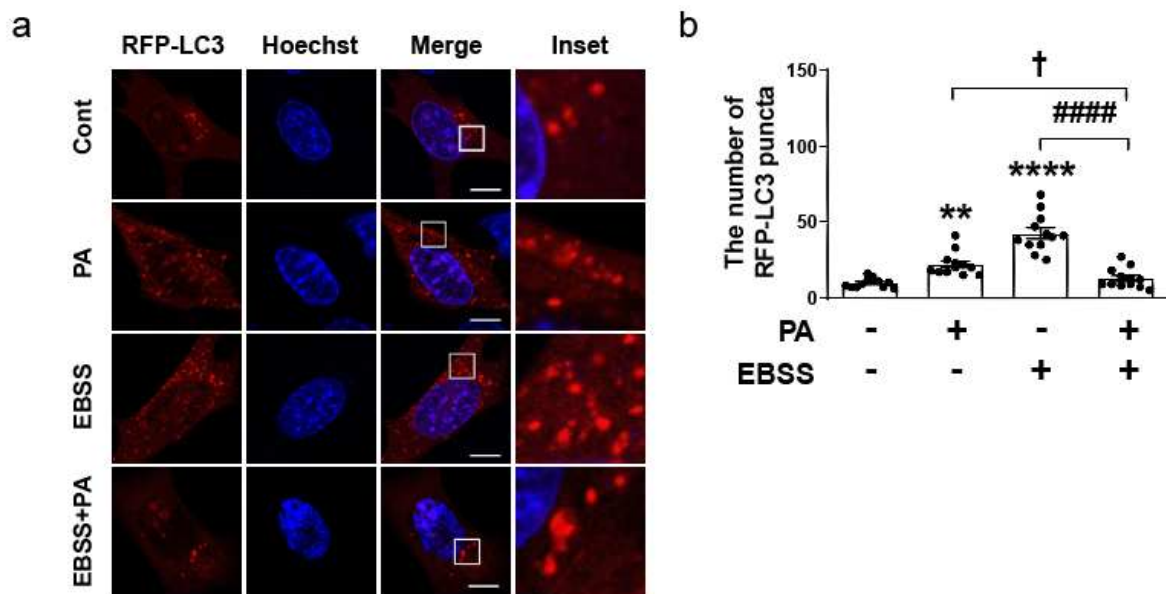


Figure 16. Palmitate inhibits EBSS-induced increase of the number of mRFP-LC3 puncta in N41 cells. Cells transiently expressing mRFP-LC3 were starved in EBSS for 3 h in the presence or absence of palmitate (0.1 mM). Representative micrographs (**a**) and quantification (**b**) of the average number of mRFP-LC3 puncta (n = 12 per each group). Scale bar, 10 μ m. Data are mean \pm SEM; ** $p=0.0032$, **** $p<0.0001$ vs. control, ##### $p<0.0001$, † $p=0.0358$.

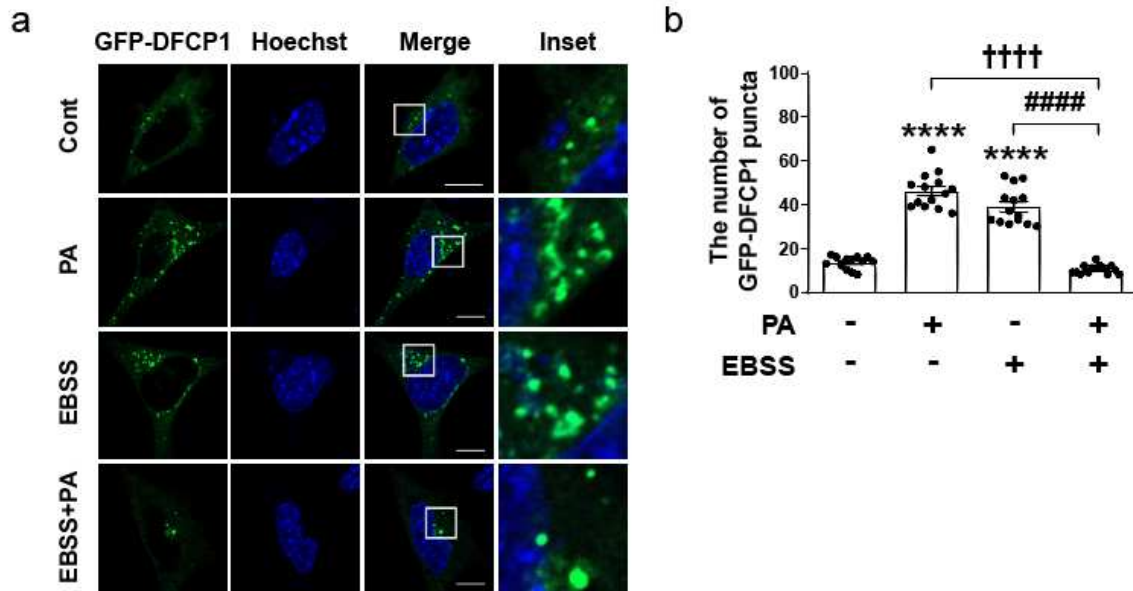
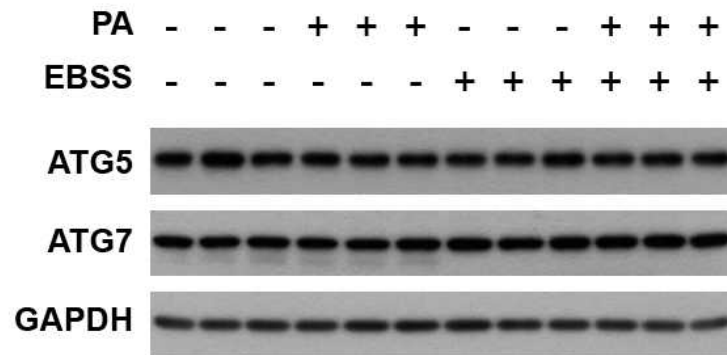


Figure 17. Palmitate inhibits EBSS-induced increase of the number of mRFP-LC3 puncta. Cells transiently expressing GFP-DFCP1 were starved in EBSS for 3 h in the presence or absence of palmitate (0.1 mM). Representative micrographs (**a**) and quantification (**b**) of the average number of GFP-DFCP1 puncta ($n = 14$ per each group). Scale bar, 10 μm . Data are mean \pm SEM; **** $p < 0.0001$ vs. control, ##### $p < 0.0001$, †††† $p < 0.0001$.

a



b

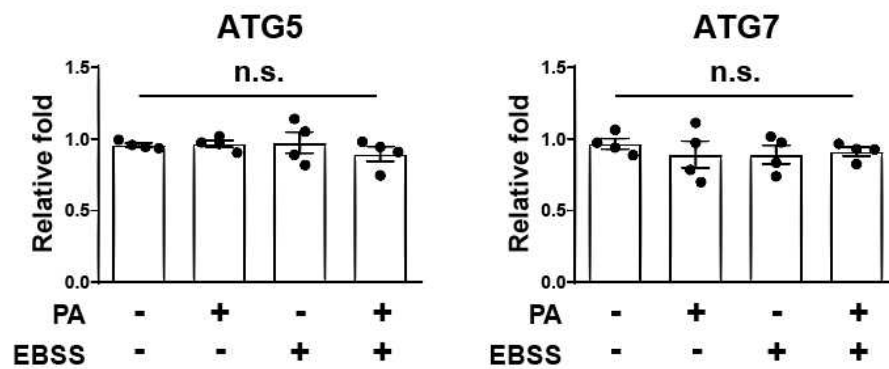


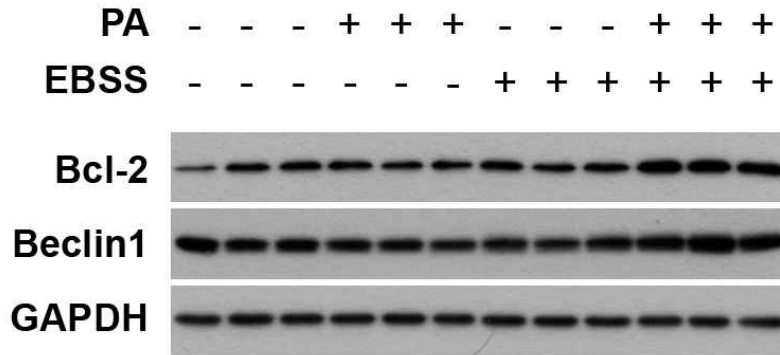
Figure 18. Palmitate does not change the levels of ATG5 and ATG7 in N41 cells. Cells were starved in EBSS for 3 h in the presence or absence of palmitate (0.1 mM). **a** and **b** Immunoblotting analysis (**a**) and quantification (**b**) of ATG5 and ATG7 (n = 4 per each group). Data are mean \pm SEM; n.s., no significant difference.

8. Inhibition of Bcl-2 ameliorates the inhibitory effect of palmitate on ER-phagy under starvation.

Bcl-2, an antiapoptotic protein, is known to inhibit Beclin1-dependent autophagy (Pattingre et al., 2005a). To examine whether palmitate-inhibited ER-phagy in starved cells is regulated by Bcl-2, I analyzed the Bcl-2 level. Interestingly, Bcl-2 and Beclin1 levels were not changed by either palmitate or EBSS, whereas co-treatment significantly increased the levels of both Bcl-2 and Beclin1 (Fig. 19a, b), suggesting that the increase in Bcl-2 might be involved in palmitate-inhibited ER-phagy. In addition, the protein level of Beclin1 was increased in co-treatment with palmitate and EBSS while the mRNA level of Beclin1 was not increased by co-treatment with palmitate and EBSS (Fig. 22), suggesting that the increased protein level of Beclin1 was due to inhibition of degradation.

To confirm whether Bcl-2 contributes to inhibition of autophagy, Bcl-2 was knocked down under EBSS or co-treatment with palmitate and EBSS conditions (Fig. 19a, b). The increase of Beclin1 under co-treatment of palmitate and EBSS compared to EBSS was diminished in *Bcl-2* knockdown cells, indicating that the increase of Beclin1 is dependent on increased Bcl-2. In addition, a decrease in the number of GFP-DFCP1 puncta under co-treatment with palmitate and EBSS conditions was reversed by the knockdown of *Bcl-2* in the same conditions (Fig. 21a, b). These data imply that Bcl-2 contributes to inhibition of autophagy initiation by palmitate under starvation. Taken together, these data suggest that ER-phagy is inhibited by palmitate at an early stage through the upregulation of Bcl-2 under starvation.

a



b

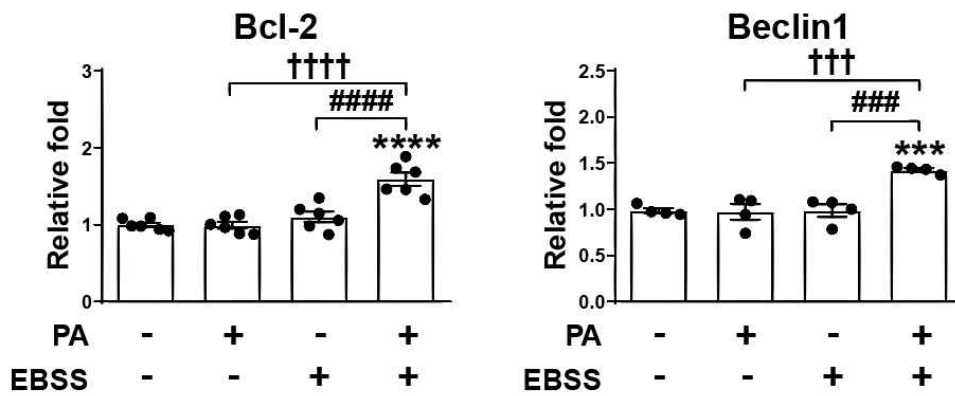
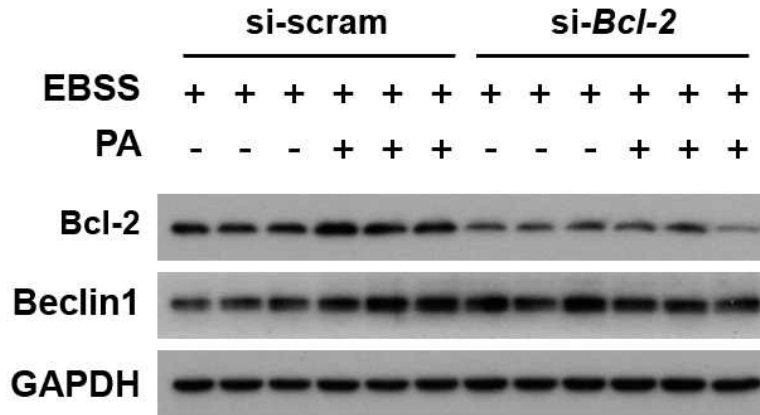


Figure 19. Palmitate increases the levels of Bcl-2 and Beclin1 under starvation in N41 cells. Cells were starved in EBSS for 3 h in the presence or absence of palmitate (0.1 mM). Immunoblotting analysis (a) and quantification (b) of Bcl-2 and Beclin1 (Bcl-2; n = 6 per each group, Beclin1; n = 4 per each group). Data are mean \pm SEM; Bcl-2; **** $p < 0.0001$ vs. control, #### $p < 0.0001$, †††† $p < 0.0001$, Beclin1; *** $p = 0.0007$ vs. control, ### $p = 0.0007$, ††† $p = 0.0005$.

a



b

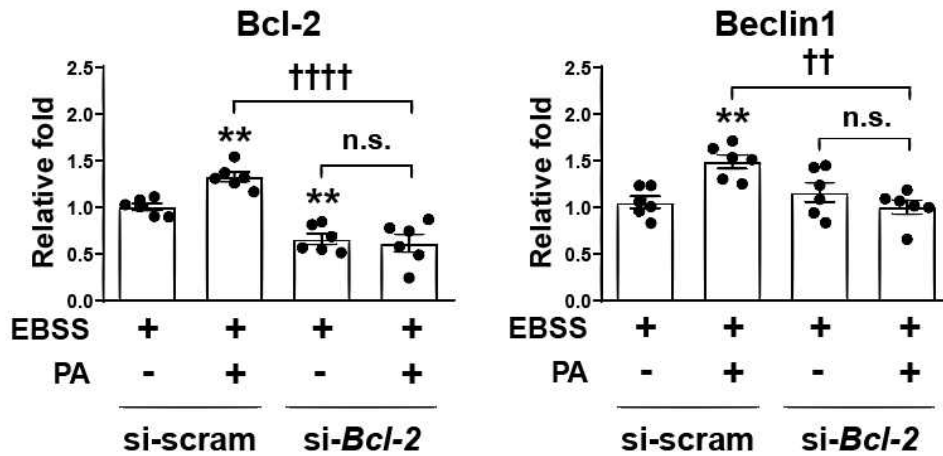


Figure 20. Palmitate does not increase the levels of Bcl-2 and Beclin1 after knockdown of *Bcl-2* under starvation in N41 cells. Cells were transfected with si-scram or si-*Bcl-2* were starved in EBSS for 3 h in the presence or absence of palmitate (0.1 mM). Immunoblotting analysis (a) and quantification (b) of Bcl-2 and Beclin1 (n = 6 per each group). Data are mean \pm SEM; Bcl-2; ** $p=0.0089$ at EBSS + PA in si-scram vs. EBSS in si-scram, ** $p=0.0054$ at EBSS in si-*Bcl-2* vs. EBSS in si-scram, †††† $p<0.0001$. Beclin1; ** $p=0.0052$ vs. EBSS in si-scram, †† $p=0.0019$. n.s., no significant difference.

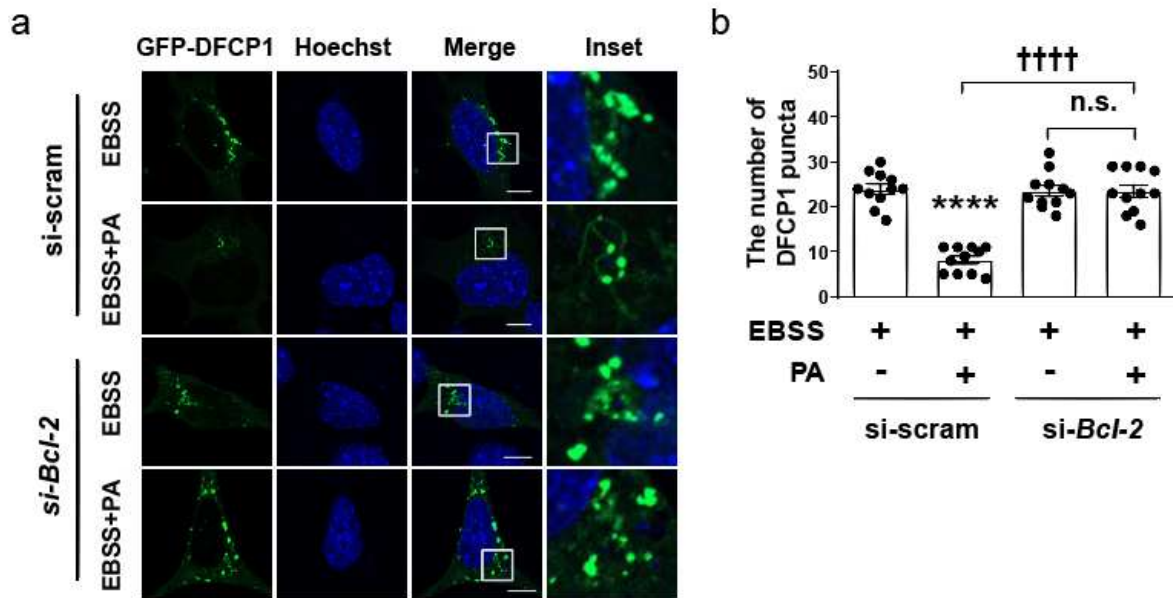


Figure 21. Palmitate inhibits ER-phagy via upregulation of Bcl-2 in N41 cells. Cells transfected with GFP-DFCP1 24 h after transfection with si-scram or si-Bcl-2 were starved in EBSS for 3 h in the presence or absence of palmitate (0.1 mM). Representative micrographs (a) and quantification (b) of the average number of GFP-DFCP1 puncta (n = 11 per each group). Scale bar, 10 μ m. Data are mean \pm SEM; **** $p < 0.0001$ vs. EBSS in si-scram, †††† $p < 0.0001$. n.s., no significant difference.

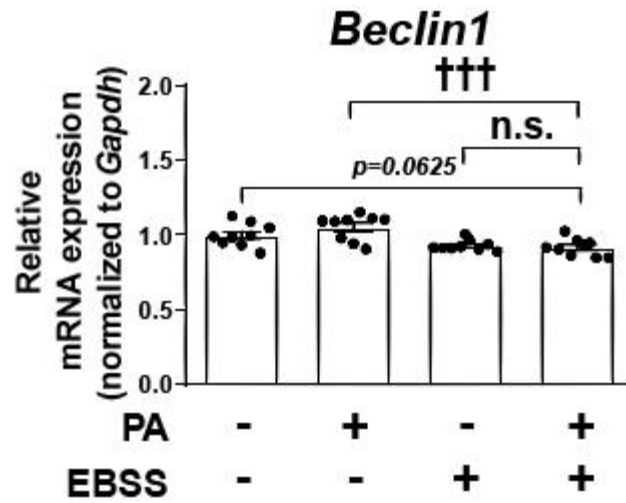


Figure 22. The mRNA level of *Beclin1* is not changed by palmitate and/or EBSS in N41 cells. Cells were starved in EBSS for 3 h in the presence or absence of palmitate (0.1 mM). **a** mRNA expression of *Beclin1* (n = 9 per each group). Data are mean \pm SEM; ††† $p=0.0008$. n.s., no significant difference.

IV. Discussion

The effects of FFAs on ER stress, autophagy, and apoptosis in the brain have been investigated mainly in the context of mimicking excess-nutrient conditions such as HFD *in vivo* (Gil-Lozano et al., 2016). However, since FFA levels are increased in the hypothalamus not only by HFD but also under starvation, the role of FFAs in both contexts needs to be further explored. Palmitate, a saturated fatty acid, induces ER stress and apoptosis in hypothalamic cells (Mayer and Belsham, 2010; Oh et al., 2019; Tse and Belsham, 2018), but the effect of palmitate on ER stress and apoptosis under starvation has not been studied. Given that starvation induces ER stress, which then upregulates ER-phagy (Smith et al., 2018), whether palmitate regulates ER stress and ER-phagy under starvation needs to be clarified. Here, I demonstrate a different role of palmitate in ER stress and ER-phagy under starvation in comparison with nutrient-rich conditions.

In this study, both palmitate and EBSS-induced starvation triggered ER stress through the ATF4-CHOP pathway, but through different upstream regulators. Under normal nutrient-rich conditions, palmitate induced ER stress through p-PERK signaling. On the other hand, EBSS degraded the three UPR sensors; therefore, starvation seems to induce ER stress in an UPR sensor-independent manner (Fig. 14a, b). Palmitate induced p-PERK to activate ATF4 while EBSS decreased all the early three UPR sensors. One paper reported that starvation uses different pathways for cell survival and death compared to ER stress and apoptosis inducers (Shin et al., 2015). Prolonged glucose starvation shows decreased PERK level and switches pathway from PERK/Akt signaling for cell survival to eIF2 α /ATF4 pathway for cell death (Shin et al., 2015). Since EBSS is severe starvation cue more than glucose starvation, EBSS might use eIF2 α /ATF4 pathway instead of PERK pathway.

Since both palmitate and EBSS increased ER stress, combined treatment could be expected to synergistically activate ER stress. However, opposite to this expectation, co-treatment with palmitate and EBSS greatly decreased the level of ER stress in comparison with that under each treatment, suggesting that palmitate differently regulates ER stress under starvation conditions in hypothalamic N41 cells.

I also demonstrated that palmitate differently regulates ER-phagy depending on nutrient status. Under nutrient-rich conditions, our data showed the existence of basal ER-phagy, which was not affected by short-term treatment with palmitate, but was impaired by prolonged palmitate treatment. Starvation, on the other hand, significantly induced ER-phagy, which accounted for half of total autophagy. Surprisingly, short palmitate treatment inhibited starvation-induced ER-phagy close to basal level (Fig. 12a, b). Overall, palmitate inhibited both ER-phagy and ER stress under starvation (Figs. 12a, b and 13a, b). Furthermore, I showed that ER-phagy precedes ER stress and is required for ER stress under starvation (Fig. 15a–d). Although many studies have reported that ER stress induces autophagy, including ER-phagy (Ding et al., 2007; Ogata et al., 2006; Qin et al., 2010; Smith et al., 2018), the opposite is also possible because excessive ER-phagy may cause ER stress (Liao et al., 2019).

One interesting finding in our study is that palmitate yields opposite levels of autophagy flux depending on treatment duration under nutrient-rich conditions. Acute and chronic exposure of cells to palmitate can elicit Ca^{2+} influx through distinct entry mechanisms with different physiological outcomes (Hoppa et al., 2009). Since autophagy can be induced or suppressed by various intracellular modulators, including Ca^{2+} (Brady et al., 2007; Criollo et al., 2007; Gao et al., 2008; Høyer-Hansen et al., 2007; Vicencio et al., 2009), I speculate that short vs. long treatment of palmitate may have different effects on intracellular Ca^{2+} signaling,

and subsequently autophagy.

One study demonstrated that long treatment with palmitate (16 h) impaired autophagy by suppressing the conversion from LC3-I to LC3-II and accumulating p62 level despite increasing the number and size of autophagosome in nutrient-rich conditions (Mir et al., 2015). Although the study showed that palmitate overwhelmingly impaired autophagy even under amino acids starvation, the short-time effect of palmitate on autophagy under starvation or the type of autophagy was not investigated. Interestingly, our data showed that short treatment with palmitate (3 h) impaired autophagy, especially ER-phagy, by inhibiting the initiation of autophagosome formation under starvation.

I propose a mechanism by which palmitate inhibits autophagosome formation to inhibit ER-phagy under starvation (Fig. 16a, b and Fig. 17a, b). Under nutrient-rich conditions, palmitate inhibits autophagy by degrading ATG5 or ATG7 protein in several cell lines (Mallik and Yammani, 2018; Nissar et al., 2017), but the effect of palmitate on the regulation of ATG genes or proteins in hypothalamic cells has not been studied. Our results show that neither ATG5 nor ATG7 is affected by palmitate under nutrient-rich or starvation conditions in hypothalamic cells (Fig. 18a, b), indicating that neither of these proteins participates in the inhibition of autophagy by palmitate.

Bcl-2 inhibits autophagy through the interaction with Beclin1 (He et al., 2012; Pattingre et al., 2005a). Therefore, modulation of Bcl-2 level can be an effective mechanism to suppress or promote autophagy (Xu et al., 2013). In our study, the levels of Bcl-2 and Beclin1 were not changed by either palmitate or EBSS-induced starvation but were increased by co-treatment with EBSS and palmitate (Fig. 19a, b). Since the mRNA level of *Beclin1* was not changed by EBSS and/or palmitate (Fig. 22) and the increased protein level of Beclin1 by

co-treatment with EBSS and palmitate was diminished in *Bcl-2* knockdown cells (Fig. 20a, b), the increase in Beclin1 protein by palmitate is likely due to Bcl-2-mediated Beclin1 stability at this conditions.

Taken together, our data demonstrate that palmitate differently regulates ER-phagy and ER stress depending on nutrient conditions (Fig. 23). Palmitate inhibits both ER-phagy and ER stress under starvation, relieving cellular stress. Further studies on the role of palmitate in the regulation of ER-phagy in the hypothalamus under fasting *in vivo* will be needed. In conclusion, our findings suggest that palmitate may work as a regulator of ER-phagy under starvation.

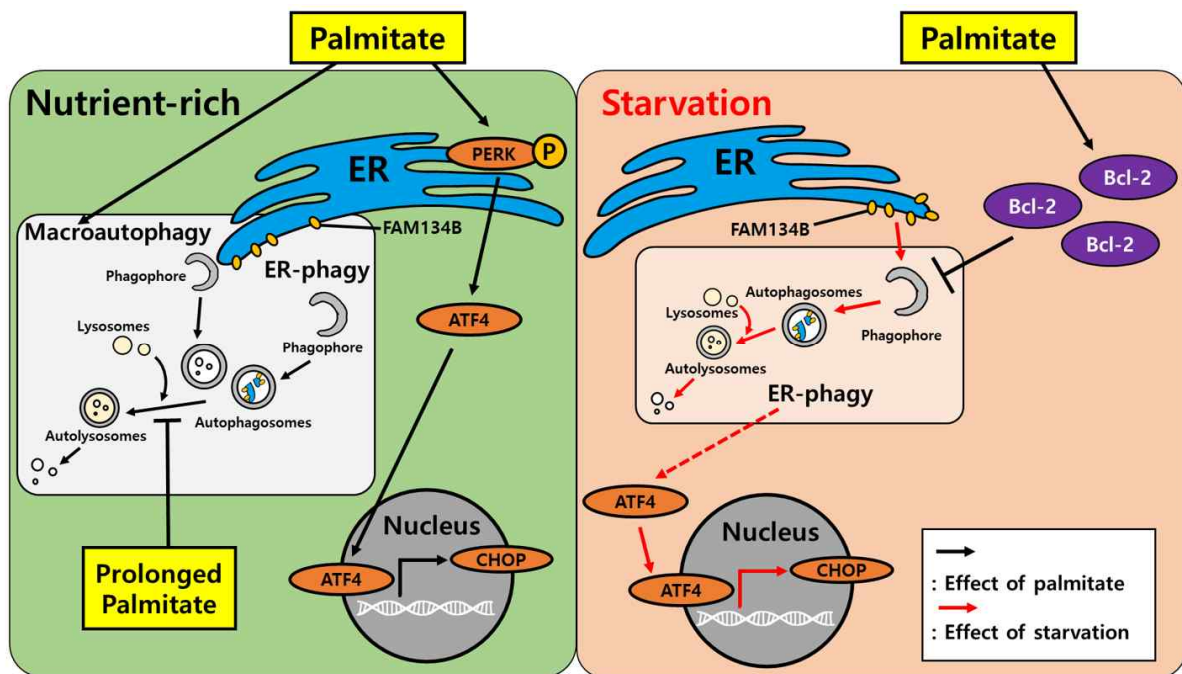


Figure 23. A schematic diagram illustrating the different roles of palmitate in ER-phagy and ER stress under nutrient-rich and starvation conditions. Palmitate induces p-PERK-mediated ER stress and autophagy, but prolonged treatment with palmitate impairs autophagy under nutrient-rich conditions. EBSS-induced starvation increases ER-phagy and ER stress, and ER-phagy precedes ER stress under these circumstances. Palmitate inhibits ER-phagy by increasing Bcl-2 and also decreases ER stress under EBSS-induced starvation.

V. Conclusion

In this study, I demonstrate the different role of palmitate on ER stress and ER-phagy under nutrient-rich and starvation conditions. Palmitate induces ER stress and autophagy at short time point, but inhibits overall autophagy including ER-phagy under starvation by preventing the autophagosome formation. Starvation itself induces ER stress and ER-phagy but both inductions are completely inhibited by co-treatment with palmitate. The inhibitory effect of palmitate on ER-phagy is dependent on the increase of Bcl-2, which inhibits autophagy by interacting with Beclin1. After the knockdown of *Bcl-2*, palmitate does not inhibit autophagosome formation under starvation, suggesting that Bcl-2 contributes to inhibition of autophagy initiation. These results imply that palmitate decreases starvation-induced cellular damage in hypothalamic cells by inhibiting ER-phagy.

VI. References

- Alzoubi, K., Abdul-Razzak, K., Khabour, O., Al-Tuweiq, G., Alzubi, M., and Alkadhi, K. (2009). Adverse effect of combination of chronic psychosocial stress and high fat diet on hippocampus-dependent memory in rats. *Behavioural brain research* *204*, 117-123.
- Axe, E.L., Walker, S.A., Manifava, M., Chandra, P., Roderick, H.L., Habermann, A., Griffiths, G., and Ktistakis, N.T. (2008a). Autophagosome formation from membrane compartments enriched in phosphatidylinositol 3-phosphate and dynamically connected to the endoplasmic reticulum. *J Cell Biol* *182*, 685-701.
- Axe, E.L., Walker, S.A., Manifava, M., Chandra, P., Roderick, H.L., Habermann, A., Griffiths, G., and Ktistakis, N.T. (2008b). Autophagosome formation from membrane compartments enriched in phosphatidylinositol 3-phosphate and dynamically connected to the endoplasmic reticulum. *The Journal of cell biology* *182*, 685-701.
- Ayton, S., Lei, P., Hare, D.J., Duce, J.A., George, J.L., Adlard, P.A., McLean, C., Rogers, J.T., Cherny, R.A., Finkelstein, D.I., et al. (2015). Parkinson's disease iron deposition caused by nitric oxide-induced loss of beta-amyloid precursor protein. *J Neurosci* *35*, 3591-3597.
- B'Chir, W., Maurin, A.C., Carraro, V., Averous, J., Jousse, C., Muranishi, Y., Parry, L., Stepien, G., Fafournoux, P., and Bruhat, A. (2013). The eIF2alpha/ATF4 pathway is essential for stress-induced autophagy gene expression. *Nucleic Acids Res* *41*, 7683-7699.
- Benoit, S.C., Kemp, C.J., Elias, C.F., Abplanalp, W., Herman, J.P., Migrenne, S., Lefevre, A.-L., Cruciani-Guglielmacci, C., Magnan, C., Yu, F., et al. (2009). Palmitic acid mediates hypothalamic insulin resistance by altering PKC-theta subcellular localization in rodents. *The Journal of clinical investigation* *119*, 2577-2589.
- Bernales, S., McDonald, K.L., and Walter, P. (2006). Autophagy counterbalances endoplasmic reticulum expansion during the unfolded protein response. *PLoS Biol* *4*, e423.
- Bernales, S., Schuck, S., and Walter, P. (2007). ER-phagy: selective autophagy of the endoplasmic reticulum. *Autophagy* *3*, 285-287.
- Bjorkoy, G., Lamark, T., Pankiv, S., Overvatn, A., Brech, A., and Johansen, T. (2009). Monitoring autophagic degradation of p62/SQSTM1. *Methods Enzymol* *452*, 181-197.
- Boden, G., and Shulman, G.I. (2002). Free fatty acids in obesity and type 2 diabetes: defining their role in the development of insulin resistance and beta-cell dysfunction. *Eur J Clin Invest* *32 Suppl 3*, 14-23.
- Brady, N.R., Hamacher-Brady, A., Yuan, H., and Gottlieb, R.A. (2007). The autophagic response to nutrient deprivation in the h1-1 cardiac myocyte is modulated by Bcl-2 and sarco/endoplasmic reticulum calcium stores. *FEBS Journal* *274*, 3184-3197.
- Chen, Q., Xiao, Y., Chai, P., Zheng, P., Teng, J., and Chen, J. (2019). ATL3 Is a Tubular ER-Phagy Receptor for

GABARAP-Mediated Selective Autophagy. *Curr Biol* 29, 846-855.e846.

Chen, X., Yi, L., Song, S., Wang, L., Liang, Q., Wang, Y., Wu, Y., and Gao, Q. (2018). Puerarin attenuates palmitate-induced mitochondrial dysfunction, impaired mitophagy and inflammation in L6 myotubes. *Life Sci* 206, 84-92.

Cho, D.H., Kim, Y.S., Jo, D.S., Choe, S.K., and Jo, E.K. (2018). Pexophagy: Molecular Mechanisms and Implications for Health and Diseases. *Mol Cells* 41, 55-64.

Choi, S.J., Kim, F., Schwartz, M.W., and Wisse, B.E. (2010). Cultured hypothalamic neurons are resistant to inflammation and insulin resistance induced by saturated fatty acids. *Am J Physiol Endocrinol Metab* 298, E1122-1130.

Cook, K.L., Soto-Pantoja, D.R., Abu-Asab, M., Clarke, P.A., Roberts, D.D., and Clarke, R. (2014). Mitochondria directly donate their membrane to form autophagosomes during a novel mechanism of parkin-associated mitophagy. *Cell Biosci* 4, 16.

Coupé, B., Leloup, C., Asiedu, K., Maillard, J., Pénicaud, L., Horvath, T.L., and Bouret, S.G. (2021). Defective autophagy in Sfl neurons perturbs the metabolic response to fasting and causes mitochondrial dysfunction. *Mol Metab* 47, 101186.

Criollo, A., Maiuri, M.C., Tasdemir, E., Vitale, I., Fiebig, A.A., Andrews, D., Molgó, J., Díaz, J., Lavandero, S., Harper, F., et al. (2007). Regulation of autophagy by the inositol trisphosphate receptor. *Cell Death and Differentiation* 14, 1029-1039.

Cuervo, A.M. (2008). Autophagy and aging: keeping that old broom working. *Trends in Genetics* 24, 604-612.

Cuervo, A.M., Bergamini, E., Brunk, U.T., Dröge, W., Ffrench, M., and Terman, A. (2005). Autophagy and aging: the importance of maintaining "clean" cells. *Autophagy* 1, 131-140.

Dalvi, P.S., Chalmers, J.A., Luo, V., Han, D.Y., Wellhauser, L., Liu, Y., Tran, D.Q., Castel, J., Luquet, S., Wheeler, M.B., et al. (2017). High fat induces acute and chronic inflammation in the hypothalamus: effect of high-fat diet, palmitate and TNF- α on appetite-regulating NPY neurons. *Int J Obes (Lond)* 41, 149-158.

Dikic, I. (2018). Open questions: why should we care about ER-phagy and ER remodelling? *BMC Biol* 16, 131.

Ding, W.X., Ni, H.M., Gao, W., Yoshimori, T., Stolz, D.B., Ron, D., and Yin, X.M. (2007). Linking of autophagy to ubiquitin-proteasome system is important for the regulation of endoplasmic reticulum stress and cell viability. *Am J Pathol* 171, 513-524.

Fumagalli, F., Noack, J., Bergmann, T.J., Cebollero, E., Pisoni, G.B., Fasana, E., Fregno, I., Galli, C., Loi, M., Solda, T., et al. (2016). Translocon component Sec62 acts in endoplasmic reticulum turnover during stress recovery. *Nat Cell Biol* 18, 1173-1184.

Fusakio, M.E., Willy, J.A., Wang, Y., Mirek, E.T., Al Baghdadi, R.J.T., Adams, C.M., Anthony, T.G., and Wek,

R.C. (2016). Transcription factor ATF4 directs basal and stress-induced gene expression in the unfolded protein response and cholesterol metabolism in the liver. *Molecular biology of the cell* *27*, 1536-1551.

Gao, W., Ding, W.X., Stolz, D.B., and Yin, X.M. (2008). Induction of macroautophagy by exogenously introduced calcium. *Autophagy* *4*, 754-761.

Geisler, S., Holmstrom, K.M., Skujat, D., Fiesel, F.C., Rothfuss, O.C., Kahle, P.J., and Springer, W. (2010). PINK1/Parkin-mediated mitophagy is dependent on VDAC1 and p62/SQSTM1. *Nat Cell Biol* *12*, 119-131.

Geng, J., Nair, U., Yasumura-Yorimitsu, K., and Klionsky, D.J. (2010). Post-Golgi Sec proteins are required for autophagy in *Saccharomyces cerevisiae*. *Mol Biol Cell* *21*, 2257-2269.

Gil-Lozano, M., Wu, W.K., Martchenko, A., and Brubaker, P.L. (2016). High-Fat Diet and Palmitate Alter the Rhythmic Secretion of Glucagon-Like Peptide-1 by the Rodent L-cell. *Endocrinology* *157*, 586-599.

Gimenez da Silva-Santi, L., Masetto Antunes, M., Mori, M.A., Biesdorf de Almeida-Souza, C., Vergílio Visentainer, J., Carbonera, F., Rabello Crisma, A., Nunes Masi, L., Massao Hirabara, S., Curi, R., et al. (2018). Brain Fatty Acid Composition and Inflammation in Mice Fed with High-Carbohydrate Diet or High-Fat Diet. *Nutrients* *10*.

Greenwood, C.E., and Winocur, G. (2001). Glucose treatment reduces memory deficits in young adult rats fed high-fat diets. *Neurobiol Learn Mem* *75*, 179-189.

Grumati, P., Morozzi, G., Hölper, S., Mari, M., Harwardt, M.-L.I.E., Yan, R., Müller, S., Reggiori, F., Heilemann, M., and Dikic, I. (2017). Full length RTN3 regulates turnover of tubular endoplasmic reticulum via selective autophagy. *eLife* *6*, e25555.

Guo, Y., Chang, C., Huang, R., Liu, B., Bao, L., and Liu, W. (2012). AP1 is essential for generation of autophagosomes from the trans-Golgi network. *J Cell Sci* *125*, 1706-1715.

Hailey, D.W., Rambold, A.S., Satpute-Krishnan, P., Mitra, K., Sougrat, R., Kim, P.K., and Lippincott-Schwartz, J. (2010). Mitochondria supply membranes for autophagosome biogenesis during starvation. *Cell* *141*, 656-667.

Hamilton, J.A., and Brunaldi, K. (2007). A model for fatty acid transport into the brain. *J Mol Neurosci* *33*, 12-17.

Hara, T., Nakamura, K., Matsui, M., Yamamoto, A., Nakahara, Y., Suzuki-Migishima, R., Yokoyama, M., Mishima, K., Saito, I., and Okano, H. (2006). Suppression of basal autophagy in neural cells causes neurodegenerative disease in mice. *Nature* *441*, 885-889.

He, C., Bassik, M.C., Moresi, V., Sun, K., Wei, Y., Zou, Z., An, Z., Loh, J., Fisher, J., Sun, Q., et al. (2012). Exercise-induced BCL2-regulated autophagy is required for muscle glucose homeostasis. *Nature* *481*, 511-515.

Henry, F.E., Sugino, K., Tozer, A., Branco, T., and Sternson, S.M. (2015). Cell type-specific transcriptomics of hypothalamic energy-sensing neuron responses to weight-loss. *eLife* *4*, e09800.

Hernández-Cáceres, M.P., Toledo-Valenzuela, L., Díaz-Castro, F., Ávalos, Y., Burgos, P., Narro, C., Peña-Oyarzun, D., Espinoza-Caicedo, J., Cifuentes-Araneda, F., Navarro-Aguad, F., et al. (2019). Palmitic Acid Reduces the Autophagic Flux and Insulin Sensitivity Through the Activation of the Free Fatty Acid Receptor 1 (FFAR1) in the Hypothalamic Neuronal Cell Line N43/5. *Front Endocrinol (Lausanne)* *10*, 176.

Hernandez, D., Torres, C.A., Setlik, W., Cebrián, C., Mosharov, E.V., Tang, G., Cheng, H.-C., Kholodilov, N., Yarygina, O., and Burke, R.E. (2012). Regulation of presynaptic neurotransmission by macroautophagy. *Neuron* *74*, 277-284.

Hoppa, M.B., Collins, S., Ramracheya, R., Hodson, L., Amisten, S., Zhang, Q., Johnson, P., Ashcroft, F.M., and Rorsman, P. (2009). Chronic palmitate exposure inhibits insulin secretion by dissociation of Ca(2+) channels from secretory granules. *Cell Metab* *10*, 455-465.

Hosokawa, N., Hara, T., Kaizuka, T., Kishi, C., Takamura, A., Miura, Y., Iemura, S., Natsume, T., Takehana, K., Yamada, N., et al. (2009). Nutrient-dependent mTORC1 association with the ULK1-Atg13-FIP200 complex required for autophagy. *Mol Biol Cell* *20*, 1981-1991.

Høyer-Hansen, M., Bastholm, L., Szyniarowski, P., Campanella, M., Szabadkai, G., Farkas, T., Bianchi, K., Fehrenbacher, N., Elling, F., Rizzuto, R., et al. (2007). Control of Macroautophagy by Calcium, Calmodulin-Dependent Kinase Kinase-β, and Bcl-2. *Molecular Cell* *25*, 193-205.

Ichimura, Y., Kirisako, T., Takao, T., Satomi, Y., Shimonishi, Y., Ishihara, N., Mizushima, N., Tanida, I., Kominami, E., Ohsumi, M., et al. (2000). A ubiquitin-like system mediates protein lipidation. *Nature* *408*, 488-492.

Ishii, M., Maeda, A., Tani, S., and Akagawa, M. (2015). Palmitate induces insulin resistance in human HepG2 hepatocytes by enhancing ubiquitination and proteasomal degradation of key insulin signaling molecules. *Arch Biochem Biophys* *566*, 26-35.

Jung, H.S., and Lee, M.S. (2010). Role of autophagy in diabetes and mitochondria. *Annals of the New York Academy of Sciences* *1201*, 79-83.

Kabeya, Y., Mizushima, N., Ueno, T., Yamamoto, A., Kirisako, T., Noda, T., Kominami, E., Ohsumi, Y., and Yoshimori, T. (2000). LC3, a mammalian homologue of yeast Apg8p, is localized in autophagosome membranes after processing. *EMBO J* *19*, 5720-5728.

Kaushik, S., Rodriguez-Navarro, J.A., Arias, E., Kiffin, R., Sahu, S., Schwartz, G.J., Cuervo, A.M., and Singh, R. (2011). Autophagy in hypothalamic AgRP neurons regulates food intake and energy balance. *Cell Metab* *14*, 173-183.

Khaminets, A., Heinrich, T., Mari, M., Grumati, P., Huebner, A.K., Akutsu, M., Liebmann, L., Stolz, A., Nietzsche, S., Koch, N., et al. (2015). Regulation of endoplasmic reticulum turnover by selective autophagy.

Nature 522, 354-358.

Kihara, A., Kabeya, Y., Ohsumi, Y., and Yoshimori, T. (2001). Beclin–phosphatidylinositol 3-kinase complex functions at the trans-Golgi network. *EMBO reports* 2, 330-335.

Kim, P.K., Hailey, D.W., Mullen, R.T., and Lippincott-Schwartz, J. (2008). Ubiquitin signals autophagic degradation of cytosolic proteins and peroxisomes. *Proc Natl Acad Sci U S A* 105, 20567-20574.

Kim, S., Kim, N., Park, S., Jeon, Y., Lee, J., Yoo, S.-J., Lee, J.-W., Moon, C., Yu, S.-W., and Kim, E.-K. (2020). Tancytic TSPO inhibition induces lipophagy to regulate lipid metabolism and improve energy balance. *Autophagy* 16, 1200-1220.

Kimura, S., Noda, T., and Yoshimori, T. (2007). Dissection of the autophagosome maturation process by a novel reporter protein, tandem fluorescent-tagged LC3. *Autophagy* 3, 452-460.

Kirkin, V., Lamark, T., Sou, Y.S., Bjorkoy, G., Nunn, J.L., Bruun, J.A., Shvets, E., McEwan, D.G., Clausen, T.H., Wild, P., et al. (2009). A role for NBR1 in autophagosomal degradation of ubiquitinated substrates. *Mol Cell* 33, 505-516.

Klionsky, D.J., Abdelmohsen, K., Abe, A., Abedin, M.J., Abeliovich, H., Acevedo Arozena, A., Adachi, H., Adams, C.M., Adams, P.D., Adeli, K., et al. (2016). Guidelines for the use and interpretation of assays for monitoring autophagy (3rd edition). *Autophagy* 12, 1-222.

Komatsu, M., Waguri, S., Chiba, T., Murata, S., Iwata, J.-i., Tanida, I., Ueno, T., Koike, M., Uchiyama, Y., and Kominami, E. (2006). Loss of autophagy in the central nervous system causes neurodegeneration in mice. *Nature* 441, 880-884.

Komatsu, M., Wang, Q.J., Holstein, G.R., Friedrich, V.L., Iwata, J.-i., Kominami, E., Chait, B.T., Tanaka, K., and Yue, Z. (2007). Essential role for autophagy protein Atg7 in the maintenance of axonal homeostasis and the prevention of axonal degeneration. *Proceedings of the National Academy of Sciences* 104, 14489-14494.

Kotoulas, O., Kalamidas, S., and Kondomerkos, D. (2006). Glycogen autophagy in glucose homeostasis. *Pathology-Research and Practice* 202, 631-638.

Kouroku, Y., Fujita, E., Tanida, I., Ueno, T., Isoai, A., Kumagai, H., Ogawa, S., Kaufman, R.J., Kominami, E., and Momoi, T. (2007). ER stress (PERK/eIF2alpha phosphorylation) mediates the polyglutamine-induced LC3 conversion, an essential step for autophagy formation. *Cell Death Differ* 14, 230-239.

Lee, J., Choi, J., Scafidi, S., and Wolfgang, M.J. (2016). Hepatic Fatty Acid Oxidation Restrains Systemic Catabolism during Starvation. *Cell Rep* 16, 201-212.

Levine, B., and Klionsky, D.J. (2004). Development by self-digestion: molecular mechanisms and biological functions of autophagy. *Dev Cell* 6, 463-477.

Liao, Y., Duan, B., Zhang, Y., Zhang, X., and Xia, B. (2019). Excessive ER-phagy mediated by the autophagy

receptor FAM134B results in ER stress, the unfolded protein response, and cell death in HeLa cells. *J Biol Chem* 294, 20009-20023.

Liu, C., Yan, D.-Y., Wang, C., Ma, Z., Deng, Y., Liu, W., and Xu, B. (2020). IRE1 signaling pathway mediates protective autophagic response against manganese-induced neuronal apoptosis in vivo and in vitro. *Science of The Total Environment* 712, 136480.

Mallik, A., and Yammani, R.R. (2018). Saturated fatty acid palmitate negatively regulates autophagy by promoting ATG5 protein degradation in meniscus cells. *Biochem Biophys Res Commun* 502, 370-374.

Maric, T., Woodside, B., and Luheshi, G.N. (2014). The effects of dietary saturated fat on basal hypothalamic neuroinflammation in rats. *Brain Behav Immun* 36, 35-45.

Marvyn, P.M., Bradley, R.M., Button, E.B., Mardian, E.B., and Duncan, R.E. (2015). Fasting upregulates adipose triglyceride lipase and hormone-sensitive lipase levels and phosphorylation in mouse kidney. *Biochem Cell Biol* 93, 262-267.

Mayer, C.M., and Belsham, D.D. (2010). Palmitate attenuates insulin signaling and induces endoplasmic reticulum stress and apoptosis in hypothalamic neurons: rescue of resistance and apoptosis through adenosine 5' monophosphate-activated protein kinase activation. *Endocrinology* 151, 576-585.

Melo, H.M., Seixas da Silva, G.d.S., Sant'Ana, M.R., Teixeira, C.V.L., Clarke, J.R., Miya Coreixas, V.S., de Melo, B.C., Fortuna, J.T.S., Forny-Germano, L., Ledo, J.H., et al. (2020). Palmitate Is Increased in the Cerebrospinal Fluid of Humans with Obesity and Induces Memory Impairment in Mice via Pro-inflammatory TNF- α . *Cell Reports* 30, 2180-2194.e2188.

Meng, Q., and Cai, D. (2011). Defective hypothalamic autophagy directs the central pathogenesis of obesity via the IkappaB kinase beta (IKKbeta)/NF-kappaB pathway. *J Biol Chem* 286, 32324-32332.

Milanski, M., Degasperi, G., Coope, A., Morari, J., Denis, R., Cintra, D.E., Tsukumo, D.M., Anhe, G., Amaral, M.E., Takahashi, H.K., et al. (2009). Saturated fatty acids produce an inflammatory response predominantly through the activation of TLR4 signaling in hypothalamus: implications for the pathogenesis of obesity. *J Neurosci* 29, 359-370.

Minokoshi, Y., Alquier, T., Furukawa, N., Kim, Y.-B., Lee, A., Xue, B., Mu, J., Fofelle, F., Ferré, P., and Birnbaum, M.J. (2004). AMP-kinase regulates food intake by responding to hormonal and nutrient signals in the hypothalamus. *Nature* 428, 569-574.

Mir, S.U., George, N.M., Zahoor, L., Harms, R., Guinn, Z., and Sarvetnick, N.E. (2015). Inhibition of autophagic turnover in β -cells by fatty acids and glucose leads to apoptotic cell death. *J Biol Chem* 290, 6071-6085.

Mizushima, N., Levine, B., Cuervo, A.M., and Klionsky, D.J. (2008). Autophagy fights disease through cellular

self-digestion. *Nature* 451, 1069-1075.

Moraes, J.C., Coope, A., Morari, J., Cintra, D.E., Roman, E.A., Pauli, J.R., Romanatto, T., Carvalheira, J.B., Oliveira, A.L., Saad, M.J., et al. (2009). High-fat diet induces apoptosis of hypothalamic neurons. *PLoS One* 4, e5045.

Nakatogawa, H. (2016). Eating the ER and the nucleus for survival under starvation conditions. *Mol Cell Oncol* 3, e1073416.

Narendra, D., Tanaka, A., Suen, D.F., and Youle, R.J. (2008). Parkin is recruited selectively to impaired mitochondria and promotes their autophagy. *J Cell Biol* 183, 795-803.

Nissar, A.U., Sharma, L., Mudasir, M.A., Nazir, L.A., Umar, S.A., Sharma, P.R., Vishwakarma, R.A., and Tasduq, S.A. (2017). Chemical chaperone 4-phenyl butyric acid (4-PBA) reduces hepatocellular lipid accumulation and lipotoxicity through induction of autophagy. *J Lipid Res* 58, 1855-1868.

Ogata, M., Hino, S., Saito, A., Morikawa, K., Kondo, S., Kanemoto, S., Murakami, T., Taniguchi, M., Tanii, I., Yoshinaga, K., et al. (2006). Autophagy is activated for cell survival after endoplasmic reticulum stress. *Mol Cell Biol* 26, 9220-9231.

Oh, S., Son, M., Choi, J., Choi, C.H., Park, K.Y., Son, K.H., and Byun, K. (2019). Phlorotannins from *Ecklonia cava* Attenuates Palmitate-Induced Endoplasmic Reticulum Stress and Leptin Resistance in Hypothalamic Neurons. *Mar Drugs* 17.

Oh, T.S., Cho, H., Cho, J.H., Yu, S.W., and Kim, E.K. (2016). Hypothalamic AMPK-induced autophagy increases food intake by regulating NPY and POMC expression. *Autophagy* 12, 2009-2025.

Pankiv, S., Clausen, T.H., Lamark, T., Brech, A., Bruun, J.A., Outzen, H., Overvatn, A., Bjorkoy, G., and Johansen, T. (2007). p62/SQSTM1 binds directly to Atg8/LC3 to facilitate degradation of ubiquitinated protein aggregates by autophagy. *J Biol Chem* 282, 24131-24145.

Papandreou, M.-E., and Tavernarakis, N. (2019). Nucleophagy: from homeostasis to disease. *Cell Death & Differentiation* 26, 630-639.

Pardridge, W.M., and Mietus, L.J. (1980). Palmitate and cholesterol transport through the blood-brain barrier. *J Neurochem* 34, 463-466.

Park, S., Oh, T.S., Kim, S., and Kim, E.K. (2019). Palmitate-induced autophagy liberates monounsaturated fatty acids and increases *Agrp* expression in hypothalamic cells. *Anim Cells Syst (Seoul)* 23, 384-391.

Pattingre, S., Tassa, A., Qu, X., Garuti, R., Liang, X.H., Mizushima, N., Packer, M., Schneider, M.D., and Levine, B. (2005a). Bcl-2 Antiapoptotic Proteins Inhibit Beclin 1-Dependent Autophagy. *Cell* 122, 927-939.

Pattingre, S., Tassa, A., Qu, X., Garuti, R., Liang, X.H., Mizushima, N., Packer, M., Schneider, M.D., and Levine, B. (2005b). Bcl-2 antiapoptotic proteins inhibit Beclin 1-dependent autophagy. *Cell* 122, 927-939.

- Qin, L., Wang, Z., Tao, L., and Wang, Y. (2010). ER stress negatively regulates AKT/TSC/mTOR pathway to enhance autophagy. *Autophagy* 6, 239-247.
- Rabinowitz, J.D., and White, E. (2010). Autophagy and metabolism. *Science* 330, 1344-1348.
- Reggiori, F., Shintani, T., Nair, U., and Klionsky, D.J. (2005). Atg9 cycles between mitochondria and the pre-autophagosomal structure in yeasts. *Autophagy* 1, 101-109.
- Reginato, A., Siqueira, B.P., Miyamoto, J., Portovedo, M., Costa, S.O., de Fante, T., Rodrigues, H.G., Ignácio-Souza, L.M., Torsoni, M.A., Torsoni, A.S., et al. (2020). Acute effects of fatty acids on autophagy in NPY neurones. *J Neuroendocrinol* 32, e12900.
- Rubinsztein, D.C., Marino, G., and Kroemer, G. (2011). Autophagy and aging. *Cell* 146, 682-695.
- Sainsbury, A., Cooney, G.J., and Herzog, H. (2002). Hypothalamic regulation of energy homeostasis. *Best Practice & Research Clinical Endocrinology & Metabolism* 16, 623-637.
- Sandyk, R. (1993). The relationship between diabetes mellitus and Parkinson's disease. *International journal of neuroscience* 69, 125-130.
- Schwartz, M.W., Woods, S.C., Porte, D., Jr., Seeley, R.J., and Baskin, D.G. (2000). Central nervous system control of food intake. *Nature* 404, 661-671.
- Sharma, M., Bhattacharyya, S., Sharma, K.B., Chauhan, S., Asthana, S., Abdin, M.Z., Vrati, S., and Kalia, M. (2017). Japanese encephalitis virus activates autophagy through XBP1 and ATF6 ER stress sensors in neuronal cells. *J Gen Virol* 98, 1027-1039.
- Shin, S., Buel, G.R., Wolgamott, L., Plas, D.R., Asara, J.M., Blenis, J., and Yoon, S.O. (2015). ERK2 Mediates Metabolic Stress Response to Regulate Cell Fate. *Mol Cell* 59, 382-398.
- Simonsen, A., Cumming, R.C., Brech, A., Isakson, P., Schubert, D.R., and Finley, K.D. (2008). Promoting basal levels of autophagy in the nervous system enhances longevity and oxidant resistance in adult *Drosophila*. *Autophagy* 4, 176-184.
- Singh, R., Kaushik, S., Wang, Y., Xiang, Y., Novak, I., Komatsu, M., Tanaka, K., Cuervo, A.M., and Czaja, M.J. (2009). Autophagy regulates lipid metabolism. *Nature* 458, 1131-1135.
- Smith, M.D., Harley, M.E., Kemp, A.J., Wills, J., Lee, M., Arends, M., von Kriegsheim, A., Behrends, C., and Wilkinson, S. (2018). CCPG1 Is a Non-canonical Autophagy Cargo Receptor Essential for ER-Phagy and Pancreatic ER Proteostasis. *Dev Cell* 44, 217-232.e211.
- Sprangers, F., Romijn, J.A., Endert, E., Ackermans, M.T., and Sauerwein, H.P. (2001). The role of free fatty acids (FFA) in the regulation of intrahepatic fluxes of glucose and glycogen metabolism during short-term starvation in healthy volunteers. *Clin Nutr* 20, 177-179.
- Tanida, I., Ueno, T., and Kominami, E. (2004). LC3 conjugation system in mammalian autophagy. *Int J*

Biochem Cell Biol 36, 2503-2518.

Thurston, T.L., Ryzhakov, G., Bloor, S., von Muhlinen, N., and Randow, F. (2009). The TBK1 adaptor and autophagy receptor NDP52 restricts the proliferation of ubiquitin-coated bacteria. *Nat Immunol* 10, 1215-1221.

Toth, M.L., Sigmund, T., Borsos, E., Barna, J., Erdelyi, P., Takacs-Vellai, K., Orosz, L., Kovacs, A.L., Csikos, G., Sass, M., et al. (2008). Longevity pathways converge on autophagy genes to regulate life span in *Caenorhabditis elegans*. *Autophagy* 4, 330-338.

Tse, E.K., and Belsham, D.D. (2018). Palmitate induces neuroinflammation, ER stress, and *Pomc* mRNA expression in hypothalamic mHypoA-POMC/GFP neurons through novel mechanisms that are prevented by oleate. *Mol Cell Endocrinol* 472, 40-49.

Ueno, T., Muno, D., and Kominami, E. (1991). Membrane markers of endoplasmic reticulum preserved in autophagic vacuolar membranes isolated from leupeptin-administered rat liver. *J Biol Chem* 266, 18995-18999.

van der Vaart, A., Griffith, J., and Reggiori, F. (2010). Exit from the Golgi is required for the expansion of the autophagosomal phagophore in yeast *Saccharomyces cerevisiae*. *Mol Biol Cell* 21, 2270-2284.

Vicencio, J.M., Ortiz, C., Criollo, A., Jones, A.W.E., Kepp, O., Galluzzi, L., Joza, N., Vitale, I., Morselli, E., Tailler, M., et al. (2009). The inositol 1,4,5-trisphosphate receptor regulates autophagy through its interaction with Beclin 1. *Cell Death and Differentiation* 16, 1006-1017.

Vives-Bauza, C., Zhou, C., Huang, Y., Cui, M., de Vries, R.L., Kim, J., May, J., Tocilescu, M.A., Liu, W., Ko, H.S., et al. (2010). PINK1-dependent recruitment of Parkin to mitochondria in mitophagy. *Proc Natl Acad Sci U S A* 107, 378-383.

Waterson, M.J., and Horvath, T.L. (2015). Neuronal Regulation of Energy Homeostasis: Beyond the Hypothalamus and Feeding. *Cell Metab* 22, 962-970.

Weigle, D.S., Selfridge, L.E., Schwartz, M.W., Seeley, R.J., Cummings, D.E., Havel, P.J., Kuijper, J.L., and BeltrandelRio, H. (1998). Elevated free fatty acids induce uncoupling protein 3 expression in muscle: a potential explanation for the effect of fasting. *Diabetes* 47, 298-302.

Williams, G., Bing, C., Cai, X.J., Harrold, J.A., King, P.J., and Liu, X.H. (2001). The hypothalamus and the control of energy homeostasis: Different circuits, different purposes. *Physiology & Behavior* 74, 683-701.

Wu, W., Xu, H., Wang, Z., Mao, Y., Yuan, L., Luo, W., Cui, Z., Cui, T., Wang, X.L., and Shen, Y.H. (2015). PINK1-Parkin-Mediated Mitophagy Protects Mitochondrial Integrity and Prevents Metabolic Stress-Induced Endothelial Injury. *PLoS One* 10, e0132499.

Xu, H.D., Wu, D., Gu, J.H., Ge, J.B., Wu, J.C., Han, R., Liang, Z.Q., and Qin, Z.H. (2013). The pro-survival role of autophagy depends on Bcl-2 under nutrition stress conditions. *PLoS One* 8, e63232.

Yang, L., Li, P., Fu, S., Calay, E.S., and Hotamisligil, G.S. (2010). Defective hepatic autophagy in obesity

promotes ER stress and causes insulin resistance. *Cell metabolism* *11*, 467-478.

Yla-Anttila, P., Vihinen, H., Jokitalo, E., and Eskelinen, E.L. (2009). 3D tomography reveals connections between the phagophore and endoplasmic reticulum. *Autophagy* *5*, 1180-1185.

Yoshii, S.R., and Mizushima, N. (2017). Monitoring and Measuring Autophagy. *International journal of molecular sciences* *18*, 1865.

요 약 문

팔미테이트가 시상하부 세포에서의 자가포식작용과 소포체 스트레스 조절에 미치는 역할

팔미테이트(palmitate)는 대표적인 포화지방산 중 하나로서 여러 세포에서 소포체 스트레스(ER stress)와 자가포식작용(autophagy)을 일으키는 것으로 잘 알려져있다. 지속적인 고지방 식이는 시상하부의 지방산 농도를 올리고, 이는 비만이나 대사장애로 이어진다. 흥미롭게도 팔미테이트를 포함한 지방산 농도는 굶주린 상태에서도 올라가는데 이 때 올라간 지방산은 여러 신체 부위에서 주로 연료로 쓰이나, 뇌 특히 시상하부에서 어떤 역할을 하는지에 대해서는 연구가 거의 되지 않았다. 본 논문에서는 시상하부 세포에 그냥 팔미테이트를 처리했을 때와 기아 조건(starvation)을 준 뒤 팔미테이트를 처리했을 때 각각 팔미테이트가 소포체 스트레스와 자가포식에 어떤 영향을 미치는지를 연구하였다. 시상하부 세포에 팔미테이트를 처리하면 소포체 스트레스와 자가포식작용이 일어나지만 팔미테이트 처리시간이 길어지면 자가포식작용이 망가지는 것을 확인하였다. 시상하부 세포를 기아 상태로 만들면 소포체를 타겟으로 한 자가포식, 즉 소포체 자가포식(ER-phagy)이 일어나고 이 소포체자가포식은 소포체 스트레스에 선행된다. 놀랍게도 시상하부 세포를 굶길 때 팔미테이트를 함께 처리하면 기아로 인해 일어나던 소포체자가포식이 자가포식의 시작 단계인 자가포식체(autophagosome)형성 단계부터 저해되어 자가포식체 개수가 현저히 감소되었다. 소포체자가포식이 감소하였기 때문에 소포체자가포식 뒤에 일어나던 소포체 스트레스 또한 함께 감소하는 것을 확인하였고, 이 과정에서 항자가포식인자 중 하나인 Bcl-2 라는 단백질이 증가하는 것을 관찰하였다. 뇌 다운(knockdown)실험을 통해 Bcl-2 양을 감소시켰을 때 팔미테이트가 기아로 인해 일어

난 소포체자가포식을 막는 정도가 줄어들었고, 이에 따라 Bcl-2 가 팔미테이트가 기아로 인한 소포체자가포식을 줄이는 데에 중추적인 역할을 한다는 것이 증명되었다. 팔미테이트 처리 혹은 굶주림 조건이 각각 단독으로는 소포체 스트레스를 올리는 사실에 비추어보았을 때, 이 두 조건을 함께 처리하였을 때 소포체 스트레스가 줄어든다는 것은 팔미테이트가 기아 상태라는 특정한 상황에서는 소포체 스트레스를 다르게 조절할 수 있다는 가능성을 시사한다. 영양 결핍 상태의 시상하부 세포에서 팔미테이트가 소포체자가포식과 소포체 스트레스를 줄이는 효과를 증명한 본 연구가 앞으로 시상하부 세포의 소포체자가포식 연구에 도움이 되기를 기대한다.

핵심어: 시상하부, 자가포식작용, 소포체포식작용, 소포체 스트레스, 지방산, 기아